①

Theoretical study of small tunnel junctions

（和訳：微小トンネル接合の理論的研究）

上田 正仁

ＮＴＴ基礎研究所

①

Theoretical study of small tunnel junctions

（和訳： 微小トンネル接合の理論的研究）

上田 正仁

ＮＴＴ基礎研究所

Acknowledgments

It is my pleasure to acknowledge the kind and generous assistance that has been offered throughout the preparation of this work. Without their help, this work would not have been possible.

The author is particularly grateful to Professor Hidetoshi Fukuyama and Professor Tsuneya Ando for their instructions and encouragements of this work. The author wishes to express his deep gratitude to Dr. Yoshihisa Yamamoto of Nippon Telegraph and Telephone Corporation (NTT) Basic Research Laboratories for his helpful discussions and support of this work. The author greatly appreciates Dr. Susumu Kurihara and Mr. Noriyuki Hatakenaka for stimulating discussions.

This work was initiated and completed at NTT Basic Research Laboratories. The author greatly appreciates Dr. Yoshinori Kato (former Executive Director), Dr. Tatsuya Kimura (Executive Director), Dr. Akihiro Hashimoto (former Executive Manager of Information Science Laboratory), Dr. Kazuhiro Kakehi (Executive Manager of Information Science Research Laboratories), and Dr. Yoshiji Horikoshi (Executive Manager of Physical Science Research Laboratory) for their support and encouragement of this work.

Finally, the author would like to thank his wife Yuko Ueda for her help, patience and dedication that have been offered to him for years.

List of Publications of Author's

1. M. Ueda, M. Kuwata, N. Nagasawa, T. Urakami, Y. Takiguchi and Y. Tsuchiya: "Picosecond time-resolved photoelectric correlation measurement with a photon-counting streak camera" Opt. Comm. **65**, 315 - 318 (1988).

2. M. Ueda: "Expressions of various joint probability distribution of photoelectrons in terms of a photocount distribution $P(n; t_1, t_2)$" Phys. Rev. A **38**, 2937 - 2942 (1988).

3. Y. Yamamoto, S. Machida, K. Watanabe, K. Igeta, M. Ueda and H. A. Haus: "Generation and quantum nondemolition measurement of number-phase squeezed states of light" Eleventh international conference on atomic physics (Paris, 1988).

4. M. Ueda: "Probability-density-functional description of photoelectron statistiscs" Phys. Rev. A **39**, 1096 - 1108 (1989).

5. M. Ueda: "Probability-density-functional description of quantum photodetection processes" Quantum Optics **1**, 131-151 (1989).

6. M. Ueda, N. Imoto and T. Ogawa: "Quantum theory for continuous photodetection processes" Phys. Rev. A **41**, 3875-3890 (1990).

7. M. Ueda: "A nonequilibrium open-system theory for continuous photodetection processes: probability-density-functional description" Phys. Rev. A **41**, 3891-3904 (1990).

8. N. Imoto, M. Ueda and T. Ogawa: "A microscopic theory of continuous measurement of photon number" Phys. Rev. A **41**, 4127-4130 (1990).

9. M. Ueda, N. Imoto and T. Ogawa: "Continuous state reduction of correlated photon fields in photodetection processes" Phys. Rev. A **41**, 6331-6344 (1990).

10. M. Ueda and Y. Yamamoto: "An exact time-domain description of the crossover from random to Coulomb-regulated single-electron-tunneling oscillations" Phys. Rev. B **41**, 3082-3086 (1990).

11. M. Ueda: "Probability-density-function description of mesoscopic normal tunnel junctions" Phys. Rev. B **42**, 3087-3099 (1990).

12. N. Imoto, M. Ueda and T. Ogawa: "Theory of non-ideal quantum-nondemolition measurement and continuous state reduction of photonic state in view of unsharp measurement" Symposium on the foundations of modern physics (Joensuu, Finland, 1990).

13. T. Ogawa, M. Ueda and N. Imoto: "Measurement-induced oscillations of a highly squeezed state between super- and sub-Poissonian photon statistics" Phys. Rev. Lett. (to be published).

14. T. Ogawa, M. Ueda and N. Imoto: "Generation of Schrödinger's cat state by continuous photodetection" Phys. Rev. A (to be published).

15. M. Ueda: "Standard quantum limit and squeezing of mesoscopic tunneling current" 19th International conference on low temperature physics (Brighton, U.K., 16-22 August 1990) Physica B **165** & **166** 981-982 (1990).

16. M. Ueda and N. Hatakenaka: "Theory of mesoscopic tunnel junctions — from shot noise to standard quantum limit –" Phys. Rev. B (to be published).

17. M. Ueda and S. Kurihara: "Quantum theory of ultrasmall tunnel junctions" Proceedings of the LT-19 Satellite Workshop on Macroscopic Quantum Phenomena, edited by T. D. Clark (World Scientific, Singapore, 1990).

18. M. Ueda and S. Kurihara: "Infrared Divergence in Single-Electron Tunneling" Phys. Rev. Lett. (submitted).

19. M. Kitagawa and M. Ueda: "Squeezed Spin State" Phys. Rev. Lett. (submitted).

Contents

1. Introduction

Recent advances in microfabrication techniques, cryogenics, and precision measurement have opened up new possibilities in the physics of ultrasmall tunnel junctions having capacitance less than 10^{-15} F. Such junctions, if operated below 1 K under an appropriate bias condition, produce tunneling events that are correlated in time and/or in space.[1] Considerable attention, both experimentally and theoretically, has been paid to the correlated single-electron tunneling (SET), and several important applications such as single-electron transistors have been proposed.[2] Furthermore, some fundamental aspects in tunneling phenomena, like the effect of the electromagnetic environment on tunneling[3]–[6] and the traversal time for tunneling,[7] have seen a remarkable resurgence of interest in recent years because they are at the cutting edge of the present measurement technology. This paper develops two theories that were motivated by the impressive state of the art of the microjunction physics.

The discovery of the elementary charging effect in small tunnel junctions dates back to early 1960's,[8]–[11] when the dc conductance of low-capacitance tunnel junctions was found to be substantially suppressed at low temperatures. However, it was noticed only recently[12] that tunneling events become correlated in time and/or in space if the change in the junction charge due to the *discrete* tunneling across the energy barrier is supplemented by *continuous* recharging of the junction from the external circuit. This remarkable prediction immediately attracted attention under the name of *Coulomb blockade of tunneling* and it was soon confirmed experimentally in various configurations such as double junctions,[13]–[15] linear arrays of junctions,[16] and scanning-tunneling microscope (STM).[17][18]

Conventional treatments of the dynamics of mesoscopic normal tunnel junctions mainly reduce the problem to a stochastic equation and finally resort to computer simulation.[12][20]–[22] The first half of this paper proposes a new method of solving this problem in a fully analytic manner.[23]–[26] Analytic expressions of the charge distribution across the junction and current-voltage characteristics are obtained under an arbitrary bias condition. In particular, it is found that even for the ideal constant-current operation at zero temperature the degree of randomness of SET events, which is defined as the ratio of the standard deviation of tunneling lifetimes to their mean value, never reaches zero but only attains a minimum of $\sqrt{(4-\pi)R_T C I_{dc}/e}$, where

e is the electronic charge, R_T is the tunnel resistance, C is the junction capacitance, and I_{dc} is the bias current. This limit, which we shall refer to as the *standard quantum limit*, is shown to originate from the time-energy uncertainty principle that is inherent in quantum-mechanical tunneling. The whole analysis in the first half is based on a simple formula for the semiclassical tunneling rate. By so doing, however, a critical point is reached where the semiclassical theory of Coulomb blockade manifestly breaks down.

The semiclassical theory of Coulomb blockade is well confirmed in multijunction configurations,[13] but its applicability to single junctions is still problematic[27]–[29] because it is very difficult for a single junction to be completely free from parasitic capacitance. Motivated by such experimental difficulties, several theories have been proposed[3]–[6] that attempt to describe the effect of the electromagnetic environment on Coulomb blockade.

The second half of this paper predicts that the many-body final-state interaction in the electrodes, which sets in upon tunneling, plays the role of the "Fermi-surface" environment.[30][31] It is shown that a sudden change in the localized Coulomb potential due to tunneling causes infrared-divergent excitation of electron-hole pairs near the Fermi surface. Such an infrared anomaly in the density of final states available for tunneling is shown to renormalize the tunneling rate in a singular way. The zero-bias anomaly in small tunnel junctions is shown to have the same physical origin, where the anomalous power exponent is determined consistently with the Friedel sum rule. This is the first (at least, in the field of Coulomb blockade) attempt to incorporate the electrical relaxation inside the electrodes into the tunneling process, and hopefully it will resolve the controversial issue over the relativistic cutoff of the capacitance advocated by Büttiker and Landauer[7].

This paper is organized as follows. Section 2 provides a brief overview of the conventional theory of Coulomb blockade and the effect of the electrodynamic environment on it. This section is intended to provide minimal background for later discussion. Section 3 proposes a new analytic approach to ultrasmall normal tunnel junctions. With this method, an analytic expression of the current-voltage characteristic of small tunnel junctions is obtained under an arbitrary bias condition. The relationship of the proposed method to the conventional master-equation approach is also discussed. Section 4 discusses noise characteristics of small tunnel junctions under various bias conditions. It is shown that SET events exhibits a crossover

from random shot noise (represented by the Schottky formula) to Coulomb-regulated oscillations. This regularity, however, is shown to have a fundamental upper bound represented by the standard quantum limit. Section 5 discusses that this limit does not originate from current or thermal fluctuations but from the time-energy uncertainty principle that is inherent in quantum-mechanical tunneling. Section 6 develops a microscopic theory of Coulomb suppression and zero-bias anomaly of tunneling conductance under the influence of the Fermi-surface environment. Section 7 discusses and summarizes the main results of the present paper. Some complicated algebraic manipulations are relegated to appendices to avoid digressing from the main subject.

2. Orthodox theory and beyond

This section briefly overviews the present state of the art in the physics of mesoscopic normal tunnel junctions to provide a background for later discussions.

2.1. Principle of Coulomb blockade

Let us consider a tunnel junction made up of two normal metal electrodes and an energy barrier sandwiched by them. Owing to its wave nature (Fig. 1(a)), an electron can pass through an energy barrier that a classical particle could not penetrate. This is all that textbook quantum mechanics tells us. In fact, electron tunneling is accompanied by a transfer of charge that is quantized in units of the electronic charge e. As a result, each tunneling event occurs at an energy cost of $\frac{e}{C}\left(\frac{e}{2}-Q\right)$ (Fig. 1(b)), where C is the electrostatic capacitance of the junction and Q is the charge that was accumulated on the junction before the tunneling event occurred. For macroscopic junctions this energy cost is overwhelmed by the masking thermal energy k_BT.[32] This is why the particle nature of an electron (i.e., quantization of charge) has not been manifest in conventional tunneling phenomena. However, when the electrostatic capacitance of the junction is less than 1 $fF(10^{-15}F)$, the equivalent temperature of the energy cost becomes more than 1 K. If we cool the temperature of the junction to below 1 K, the forward tunneling event will be suppressed for $Q < \frac{e}{2}$. Similarly, the backward tunneling event will be suppressed for $Q > -\frac{e}{2}$. At absolute zero temperature, in particular, tunneling events (both forward and backward) are completely inhibited for $|Q| < \frac{e}{2}$. This is the principle of Coulomb blockade. With this principle, we can control tunneling current at the level of a single electron, provided that we can properly manipulate the accumulated charge Q by an external circuit.

2.2. Single-electron-tunneling (SET) oscillations

What happens if an ultrasmall tunnel junction is driven by a constant-current source with current I (Fig. 2(a))? A tunneling event occurs only if the accumulated charge Q exceeds $\frac{e}{2}$. Once this occurs, however, it will be inhibited until Q again exceeds $\frac{e}{2}$ (Fig. 2(b)). Tunneling

events thus occur almost regularly at an average interval of $\tau = \frac{e}{I}$ (Fig. 2(c)). Accordingly, the voltage across the junction oscillates with frequency $f = \frac{I}{e}$. These oscillations are termed single-electron-tunneling (SET) oscillations. As seen from the above discussion, SET oscillations are based on two distinct mechanisms of charge transfer — that is, *discrete* transfer of the quantized electronic charge across the tunnel barrier and *continuous* transfer of the electrostatic charge from outside the tunnel junction.

2.3. Tunneling rate

Now let us start with a discussion of the tunneling rate in an ultrasmall normal-metal tunnel junction. Suppose that the accumulated charge (or voltage) across the junction is given by Q (or V). Then the forward tunneling rate $r(Q)$ is given by

$$r(Q) = \int_{-\infty}^{\infty} \tau^{-1}(E) D_R(E) D_L(E + eV - \frac{e^2}{2C}) f_F(E) \left[1 - f_F\left(E + eV - \frac{e^2}{2C}\right)\right] dE, \qquad (2.1)$$

where $\tau^{-1}(E)$ is the elastic tunneling rate, $D_R(E)$ [or $D_L(E)$] is the density of states in the right (or left) electrode, and $f_F(E)$ is the equilibrium Fermi distribution

$$f_F(E) = \frac{1}{1 + \exp\left(\frac{E}{k_B T}\right)}. \qquad (2.2)$$

We note that Eq. (2.1) reduces to the corresponding formula for macroscopic tunnel junctions[33] when the single-electron charging energy $\frac{e^2}{2C}$ may be neglected. This minor modification, however, leads to a major change in the physics of small tunnel junctions. We note that the factor $f_F(E)\left[1 - f_F\left(E + eV - \frac{e^2}{2C}\right)\right]$ contributes significantly to the integral only within range $\left|eV - \frac{e^2}{2C}\right|$. This energy range is typically of the order of millielectronvolts, while the Fermi energy E_F of conduction electrons is of the order of electronvolts. Therefore, the elastic tunneling rate and the densities of state may be well approximated by their values at the Fermi energy. We thus obtain

$$r(Q) = \frac{1}{eR_T C} \frac{Q - \frac{e}{2}}{1 - \exp\left[-\frac{e}{Ck_B T}\left(Q - \frac{e}{2}\right)\right]}, \qquad (2.3)$$

where

$$R_T = \frac{1}{e^2 \tau^{-1}(E_F) D_R(E_F) D_L(E_F)} \qquad (2.4)$$

defines the tunnel resistance because it gives the resistance of a tunnel junction when a constant voltage is applied across the junction.[33] When $k_BT \ll \frac{e^2}{2C}$, Eq. (2.3) reduces to

$$r(Q) = \begin{cases} 0 & \text{if } Q \leq \frac{e}{2}, \\ \frac{Q-\frac{e}{2}}{eR_TC} & \text{otherwise.} \end{cases} \tag{2.5}$$

That is, the forward tunneling events are completely inhibited until the accumulated charge exceeds $\frac{e}{2}$.

Similarly, the backward tunneling rate, $l(Q)$, is given by

$$l(Q) = \frac{1}{eR_TC} \frac{Q+\frac{e}{2}}{\exp\left[\frac{e}{Ck_BT}\left(Q+\frac{e}{2}\right)\right]-1}. \tag{2.6}$$

When $k_BT \ll \frac{e^2}{2C}$, Eq. (2.6) reduces to

$$l(Q) = \begin{cases} 0 & \text{if } Q \geq -\frac{e}{2}, \\ -\frac{Q+\frac{e}{2}}{eR_TC} & \text{otherwise.} \end{cases} \tag{2.7}$$

That is, the backward tunneling events are completely inhibited for $Q \geq -\frac{e}{2}$.

Note that Eqs. (2.5) and (2.7) reconfirm the discussion in Sec. 2.1.

2.4. Standard approaches to mesoscopic normal tunnel junctions

A standard approach to mesoscopic normal tunnel junctions usually resorts to computer simulation using Eqs. (2.5) and (2.7) (or Eqs. (2.3) and (2.6)). Suppose that an ultrasmall tunnel junction is driven by a time-dependent external current $I(t)$. Then the charge $Q(t)$ on the junction evolves in time according to the following stochastic equations:[20]

$$Q(t+dt) = \begin{cases} Q(t) + I(t)dt - e & \text{for forward tunneling,} \\ Q(t) + I(t)dt + e & \text{for backward tunneling,} \\ Q(t) + I(t)dt & \text{for no tunneling,} \end{cases} \tag{2.8}$$

where the probabilities are respectively given by $r(Q(t))dt$, $l(Q(t))dt$, and $1 - (r(Q(t)) + l(Q(t)))dt$, and the time step dt is taken to be so small that the probability of more than one tunneling event being registered during it can be neglected. With Eq. (2.8) one can perform computer simulation for the time evolution of $Q(t)$ $\left(\text{or voltage } V(t) \equiv \frac{Q(t)}{C}\right)$ and obtain a voltage spectrum by Fourier transforming it.

From the same equations (2.5) and (2.7) one can construct a master equation for $P(Q,t)$, the probability density of Q, as[12]

$$\begin{aligned}\frac{\partial}{\partial t}P(Q,t) = \quad & -I(t)\frac{\partial}{\partial Q}P(Q,t) + r(Q+e)P(Q+e,t) + l(Q-e)P(Q-e,t) \\ & -[r(Q)+l(Q)]\,P(Q,t) + \frac{1}{CR_S}\frac{\partial}{\partial Q}[P(Q,t)Q] \\ & +\frac{k_BT}{R_S}\frac{\partial^2}{\partial Q^2}P(Q,t), \end{aligned} \tag{2.9}$$

where the last term represents thermal noise generated in the shunt (or source) resistance R_S. The master equation gives the same results as the computer simulation. Furthermore, the master-equation approach gives us information about analytic behavior of $P(Q,t)$, but it is very difficult to obtain an exact solution except for very specific cases.

2.5. Physical meaning of fractional charge

In Sec. 2.2, it was stated that SET oscillations are based on two distinct mechanisms of continuous and discrete charge transfer. Section 2.3 showed that tunneling is Coulomb-blocked for $|Q| < \frac{e}{2}$. But how is it possible to think of charge smaller than the minimum unit of electricity e ? This puzzle is resolved by noting that Q is not necessarily a charge transferred through some cross-section of the current leads, but that it is defined by equating the electrostatic energy of the junction to $\frac{Q^2}{2C}$. The electrostatic energy of the junction is a *collective* Coulomb energy formed by all the conduction electrons and positive ions in the two electrodes. The magnitude of Q is therefore proportional to the relative displacement between the center of mass of all the conduction electrons, G_n, and that of all the positive ions, G_p (Fig. 3). Because of the huge number of conduction electrons, the position of their center of gravity can take almost continuous values, and hence so can Q.

2.6. Effects of the electromagnetic (EM) environment on Coulomb blockade

The orthodox theory of Coulomb blockade has been well verified in multijunction configurations but its applicability to single junctions is still questionable, for it is, in practice, very

difficult for a single junction to be free from the stray (i.e., parasitic) capacitance C_S. In fact, it is estimated to be as much as

$$C_S\,[fF] \sim \frac{1}{30}\lambda\,[\mu m], \tag{2.10}$$

where λ is the effective range of distances within which a tunneling electron interacts with the EM environment (λ is expressed in micrometers). However, there has been controversy over how far a tunneling electron probes its EM environment. Büttiker and Landauer[7] claim that a tunneling electron can probe the environment at distances $r < c\tau_t$, where c is the velocity of light and τ_t is the traversal time for tunneling. On the contrary, according to Nazarov's theory[3] the effective interaction extends to $r < \hbar c/\Delta E$ on the grounds that a tunneling electron should probe its EM environment for a period not less than $\hbar/\Delta E$ in order to corroborate that the energy gap ΔE really exists, where $\Delta E \equiv \max\{eV, k_B T\}$ and V is the voltage across the barrier. A recent experiment[27][34] seems to support Nazarov's interpretation. This section presents a brief summary of as much of the state-of-the-art study on this issue as is relevant to later discussion.

A. Uncertainty relationship in charged-particle tunneling

The tunneling Hamiltonian H_T is given by

$$H_T = \int_{x\subset R} d^3x \int_{x'\subset L} d^3x' T(x,x')\psi^\dagger(x)\psi(x') + h.c., \tag{2.11}$$

where R and L refers to the right and left electrodes, respectively, and $\psi(x)$ is the field operator for electrons. Since electrons are charged particles, the amplitude of the tunneling Hamiltonian, $T(x,x')$, is modified to satisfy the gauge-invariant requirement. If we take the most probable trajectory for a tunneling electron, we have

$$T(x,x') = T'(x,x')\exp\left(-\frac{ie}{\hbar c}\int_x^{x'} A(z,t)dz\right), \tag{2.12}$$

where $A(z,t)$ is the vector potential. Thus the tunneling amplitude is a c-number with respect to the electron field, but with respect to the EM field it is an operator that emerges as an EM phase:

$$\phi \equiv \frac{e}{\hbar c}\int_x^{x'} A(z,t)dz = -\frac{e}{\hbar}\int_{-\infty}^{t} V^{\rm ind}(t')dt', \tag{2.13}$$

where $V^{\rm ind}(t)$ is the voltage *induced* by tunneling. In fact, Eq. (2.13) is nothing but Faraday's law:

$$V^{\rm ind}(t) = -\frac{1}{c}\frac{d\Phi}{dt}, \quad \Phi(t) = \frac{\hbar c}{e}\phi(t). \tag{2.14}$$

As early as 1929 Heisenberg pointed out that the uncertainty principle between the position and momentum of an electron inevitably leads to the existence of zero-point fluctuations of the EM field through the Lorentz equation.[35] If this applies to tunneling, there must exist a similar uncertainty relationship between the charge and flux that are induced by charged-particle tunneling.[36] Suppose that an electron is tunneling through the barrier. The tunneling current then induces the magnetic flux Φ (Faraday's law), which, in turn, exerts a back reaction on the momentum of the electron.

$$\frac{dp_z^r}{dt} = -\frac{e}{dc}\frac{d\Phi}{dt} = -\frac{\hbar}{d}\frac{d\phi}{dt}, \tag{2.15}$$

where p_z^r is the reaction part of the total momentum and d is the width of the tunnel barrier. Equation (2.15) yields

$$\Delta\phi = \frac{d}{\hbar}\Delta p_z^r. \tag{2.16}$$

On the other hand, the displacement of an electron, Δz, during the same period, dt, induces the mirror charge, ΔQ, on either side of the barrier:

$$\Delta Q = e\frac{\Delta z}{d}. \tag{2.17}$$

From Eqs. (2.16) and (2.17) we obtain

$$\Delta\phi\Delta Q = \frac{e}{\hbar}\Delta p_z^r \Delta z \geq \frac{e}{2}, \tag{2.18}$$

where the uncertainty relationship between the position and the momentum of an electron ($\Delta p_z^r \Delta z \geq \hbar/2$) is used. Since the EM field can be probed only via a charged particle, Eq. (2.18) may be put in the following way: the uncertainty relationship for a probe system (i.e., a charged particle) inevitably leads to the uncertainty relationship for a measured system (i.e., the EM field). This conclusion applies generally to any quantum measurement and sets fundamental limits on the simultaneous measurement of two noncommuting observables[37]. In operator form, Eq. (2.18) may be written as

$$[\hat{\phi}, \hat{Q}] = ie. \tag{2.19}$$

This relationship imposes a fundamental limit on the electrodynamic properties of a small tunnel junction and also blurs the effect of Coulomb blockade as discussed below.

B. Spontaneous fluctuations of the junction charge

Figure 4 (a) schematically illustrates the circuit diagram of a current-biased single junction. To observe the effect of coulomb blockade, the capacitance of the junction, C, must be smaller than 1 fF. However, the stray capacitance is usually much larger than 1 fF. Thus, the small tunnel junction is effectively driven by a voltage source as is shown in Fig. 4 (b), where the effect of the EM environment is described by a simple LC circuit. For this simple circuit, the effect of the EM environment is described by

$$H_{\rm EM} = \frac{\hat{Q}^2}{2C} + \frac{\hbar^2}{2e^2 L}\hat{\phi}^2 - \hat{Q}V. \tag{2.20}$$

This Hamiltonian describes the Coulomb charging energy on the capacitor and the magnetic energy of the self-inductance L of the leads. Let us express the charge and the EM phase in terms of the normal modes

$$\hat{Q} = \sqrt{\frac{\hbar}{2}\left(\frac{C}{L}\right)^{1/2}}(\hat{b} + \hat{b}^\dagger) + CV, \tag{2.21}$$

$$\hat{\phi} = ie\sqrt{\frac{1}{2\hbar}\left(\frac{L}{C}\right)^{1/2}}(\hat{b} - \hat{b}^\dagger). \tag{2.22}$$

The commutation relation (2.19) between $\hat{Q}$ and $\hat{\phi}$ is equivalent to

$$[\hat{b}, \hat{b}^\dagger] = 1. \tag{2.23}$$

The Hamiltonian of the EM environment thus reduces to

$$H_{\rm EM} = \hbar\omega_L\left(b^\dagger b + \frac{1}{2}\right), \tag{2.24}$$

where a constant term $\frac{1}{2}CV^2$ is omitted and

$$\omega_L = (LC)^{-\frac{1}{2}}. \tag{2.25}$$

Thus we find that the effect of the EM environment can be evaluated by using the familiar thermodynamics of a quantized harmonic oscillator. A general EM environment of an arbitrary

linear circuit with a frequency-dependent impedance can be treated, in the spirit of Leggett,[38] as a collection of LC circuits.

Due to zero-point fluctuations of the EM field, the charge of the junction spontaneously fluctuates. A straightforward calculation shows that at zero temperature[4]

$$\langle \Delta Q^2 \rangle = \langle Q^2 \rangle - \langle Q \rangle^2 = \frac{e^2}{4} \frac{\hbar \omega_L}{E_Q}, \tag{2.26}$$

where $E_Q \equiv \frac{e^2}{2C}$. This result shows that if the zero-point energy $\frac{1}{2}\hbar\omega_L$ of the EM environment is larger than the single-electron charging energy E_Q, the spontaneous fluctuations of the junction charge, $\langle \Delta Q^2 \rangle^{1/2}$, exceed $\frac{e}{2}$ and thus the effect of Coulomb blockade is substantially reduced. In general, the EM environment may be regarded as an infinite number of harmonic oscillators. The energy-level spacing $\hbar\omega_L$ at the SET frequency ω_{SET} is related to the frequency-dependent impedance $Z(\omega)$ of the environment by

$$\hbar\omega_L \sim \frac{\hbar}{CZ(\omega_{SET})}. \tag{2.27}$$

In order for the Coulomb blockade to be observed, therefore, the impedance at the relevant frequency must be large so that the tunneling electron suffers sufficient recoil as a result of exciting the EM modes.

C. Current-voltage characteristics in the presence of the EM environment

The tunneling current can be expressed as[4]

$$I(V) = \frac{1}{eR_T} \int_{-\infty}^{\infty} dE \int_{-\infty}^{\infty} dE' \{ f(E)(1 - f(E'))P(E + eV - E') - (1 - f(E))f(E')P(E' - E - eV) \}, \tag{2.28}$$

where $P(E)$ is the probability that a tunneling electron transfers energy E to the environment. It can be derived as follows. The tunneling Hamiltonian is given by

$$\hat{H}_T = \sum_{\sigma,k,q} (T_{kq}\, e^{-i\hat{\phi}} \hat{c}^\dagger_{k\sigma} \hat{c}_{q\sigma} + T^*_{kq}\, e^{i\hat{\phi}} \hat{c}^\dagger_{q\sigma} \hat{c}_{k\sigma}), \tag{2.29}$$

where $e^{i\hat{\phi}}$ represents the discrete transfer of charge due to tunneling. This can be seen by the following relation

$$e^{i\hat{\phi}} \hat{Q} e^{-i\hat{\phi}} = \hat{Q} - e. \tag{2.30}$$

The probability $P(E)$ is given by Fermi's golden rule

$$P(E) = \sum_{i,f} |\langle i|e^{i\hat{\phi}}|f\rangle|^2 \delta(E_f - E_i - E). \tag{2.31}$$

Expressing the delta function in integral form we obtain

$$P(E) = \frac{1}{2\pi\hbar} \int_{-\infty}^{\infty} \langle e^{i\phi(t)} e^{-i\phi(0)} \rangle e^{iEt/\hbar} dt. \tag{2.32}$$

Thus we find that the probability $P(E)$ is given by the equilibrium phase correlation function which can be evaluated if the spectral density of the environmental modes, $Z(\omega)$, is known. Here we will only demonstrate how the back reaction of excitation of the environmental modes by a tunneling electron recovers the semiclassical result of Coulomb blockade.

For a simple harmonic-oscillator environment as shown in Fig. 4 (b), the equilibrium phase correlation function can be evaluated using Wick's theorem to give

$$\langle e^{i\phi(t)} e^{-i\phi(0)} \rangle = e^{\langle [\phi(t)-\phi(0)]\phi(0) \rangle}. \tag{2.33}$$

Using the thermodynamics of the quantized harmonic oscillator, the exponent of the right-hand side (rhs) can be calculated as[4][39]

$$\langle [\phi(t) - \phi(0)]\phi(0) \rangle = \frac{E_Q}{\hbar\omega_L} \left\{ (\cos\omega_L t - 1) \coth \frac{\hbar\omega_L}{2k_B T} - i \sin\omega_L t \right\}. \tag{2.34}$$

When the energy-level spacing of the relevant environmental mode is much larger than the elementary charging energy, i.e., $\hbar\omega_L \gg E_Q$, a tunneling electron cannot excite environmental modes and hence suffers no recoil. In this case, the correlation function (2.34) is equal to zero and therefore $P(E) = \delta(E)$. Substituting this into Eq. (2.28), we obtain Ohm's law

$$I(V) = \frac{V}{R_T}. \tag{2.35}$$

In the opposite limit where $E_Q \gg \hbar\omega_L$, a tunneling electron can excite an infinite number of environmental modes and hence suffers a substantial recoil. In this case, the correlation function is reduced to

$$\langle [\phi(t) - \phi(0)]\phi(0) \rangle = -i\frac{E_Q}{\hbar} t, \tag{2.36}$$

and therefore $P(E) = \delta\left(E - \frac{e^2}{2C}\right)$. Substituting this into Eq. (2.28), we obtain

$$I(V) = \frac{1}{eR_T} \left[\frac{eV - \frac{e^2}{2C}}{1 - \exp\left[-\frac{1}{k_B T}\left(eV - \frac{e^2}{2C}\right)\right]} - \frac{eV + \frac{e^2}{2C}}{\exp\left[\frac{1}{k_B T}\left(eV + \frac{e^2}{2C}\right)\right] - 1} \right], \tag{2.37}$$

which at zero temperature reduces to

$$I(V) = \frac{1}{eR_T}\left[\left(eV - \frac{e^2}{2C}\right)\theta\left(eV - \frac{e^2}{2C}\right) + \left(eV + \frac{e^2}{2C}\right)\theta\left(-eV - \frac{e^2}{2C}\right)\right], \tag{2.38}$$

where θ is the Heaviside unit-step function defined by

$$\theta(Q) = \begin{cases} 1 & (Q > 0), \\ 0 & (Q < 0). \end{cases} \tag{2.39}$$

Equation (2.38) is identical to that obtained by the orthodox theory of Coulomb blockade. As seen from the above discussion, to observe the full blockade the minimum excitation energy of the environmental mode should be zero. This observation is consistent, via Eq. (2.27), with the experimental fact that the impedance seen by the junction must be high in order to observe the Coulomb blockade.

3. Probability-density-function description of mesoscopic tunnel junctions

Standard approaches described in Sec. 2.4 correctly incorporate the effects of dissipation (shunt resistance) and fluctuations (thermal noise, etc.) on tunneling characteristics and give results in excellent agreement with experiments. However, some important problems still remain to be solved: namely, an analytic expression of the charge distribution across the junction and current-voltage characteristic when there is a finite shunt resistance. In particular, which element determines the fundamental limit for the regularity of SET oscillations when the junction is driven by an ideal constant-current source ? This section develops a new analytic method of investigating the dynamics of mesoscopic normal tunnel junctions to answer these problems.[23]-[26]

3.1. Model and assumptions

Throughout this section and the following two sections a simple semiclassical model is adopted in which a normal tunnel junction with capacitance C and tunnel resistance R_T is connected in series to a voltage source with resistance R_S (Fig. 5 (a)). This model is equivalent to a current-biased shunted junction (Fig. 5 (b)), the model usually adopted in the standard approaches. We will neglect all other circuit elements such as stray capacitance and inductance. Although these elements are crucially important for experimentalists, we leave them out, nevertheless, to present the theory in its simplest possible form. Both tunnel resistance R_T and source resistance R_S are assumed to be much larger than the resistance quantum $R_Q = \frac{h}{e^2}$ in order that the quantum-mechanical energy uncertainties[40], which arise complementarily from the tunneling lifetime and the charge relaxation time, can be neglected compared to the single-electron charging energy. In particular, the condition $R_T \gg R_Q$ implies that an electron is almost always localized on one or the other side of the barrier. The traversal time for tunneling, τ_t, is assumed to be negligible compared to both the tunneling lifetime and the charge relaxation time. If the latter condition fails to be met, no Coulomb blockade would be present because the change in the junction charge due to tunneling would be completely

compensated for during the traversal time. The thermal equilibration time inside the electrodes is also assumed to be negligible. This assumption ensures the equilibrium Fermi distribution.

3.2. Definitions of various probability distributions

In Sec. 2.3, we showed that the tunneling rate depends only on the charge immediately before a tunneling event occurs and that it does not depend on any information concerning the earlier tunneling events. In general, such a process is characterized with a second-order correlation function. As such functions we introduce two kinds of probability distributions: time-interval and charge-interval distributions.

A. Time-interval distribution

Suppose that single-electron tunneling events occur at times $t_j (j = 1, 2, \cdots)$ (Fig. 6 (a)). Then the tunneling characteristics can be best described with the probability distribution of time intervals between consecutive tunneling events: $\tau_j \equiv t_{j+1} - t_j (j = 1, 2, \cdots)$. We denote this probability distribution as $P_{s11}(\tau)$.[41] That is, this quantity gives the probability density that the first subsequent tunneling event occurs τ seconds after the earlier one [Fig. 6 (b)]. In general, the more regularly tunneling events occurs, the more sharply the time-interval distribution tends to peak around the average time interval, as is schematically illustrated in Fig 6 (c). The normalization condition for $P_{s11}(\tau)$ is given by

$$\int_0^\infty P_{s11}(\tau) d\tau = 1. \tag{3.1}$$

B. Charge-interval distribution

Another important distribution is the charge-interval distribution[24] $P_{s11}(Q_i, Q_f)$ which is defined as the probability density per (unit charge)^2 that the second tunneling event occurs at charge Q_f, provided that the first one occurred at charge $Q_i + e$ (see Fig. 7). The charge-interval distribution is given by the product of (i) the initial-charge distribution $P^{\text{initial}}(Q_i)$, which gives the probability distribution of charges immediately after tunneling events occurred, and (ii) the probability density $P(Q_i, Q_f)$ that the first tunneling event occurs at charge Q_f, given that the

initial charge was Q_i:

$$P_{s11}(Q_i,Q_f) = P^{\text{initial}}(Q_i)P(Q_i,Q_f). \tag{3.2}$$

Since $P(Q_i,Q_f)$ is equal to the probability density of a tunneling event occurring at charge Q_f multiplied by the probability of no tunneling events occurring until then, it is given by

$$P(Q_i,Q_f) = \frac{r(Q_f)}{i(Q_f)} \exp\left[-\int_A^{Q_f} \frac{r(Q)}{i(Q)} dQ\right], \tag{3.3}$$

where the lower bound of integration, $A \equiv \max\left(Q_i, \frac{e}{2}\right)$, appears since for $k_BT \ll \frac{e^2}{2C}$ the Coulomb blockade completely inhibits tunneling events until the junction charge exceeds $\frac{e}{2}$; $i(Q)$ is the external current, which without current noise and tunneling events is given by

$$i(Q) = \frac{CV - Q}{CR_S}. \tag{3.4}$$

Substituting Eqs. (2.5) and (3.4) into the rhs of Eq. (3.3) yields

$$P(Q_i,Q_f) = \frac{1}{e}\frac{R_S}{R_T}\frac{Q_f - \frac{e}{2}}{CV - Q_f}\left[\frac{CV - Q_f}{CV - A}\right]^{\frac{R_S}{R_T}\left(\frac{CV}{e}-\frac{1}{2}\right)} \exp\left[\frac{1}{e}\frac{R_S}{R_T}(Q_f - A)\right]. \tag{3.5}$$

It is easy to see that this equation (or, in general, Eq. (3.3)) satisfies the normalization condition

$$\int_A^{CV} P(Q_i,Q_f)dQ_f = 1. \tag{3.6}$$

Equation (3.5) includes both junction parameters (C, R_T) and circuit parameters (V, R_S) in a manner that cannot be disentangled. This is one of the unique features of small tunnel junctions: since they exhibit very sensitive, nonlinear response to an external macroscopic system, one cannot, in general, eliminate the external macroscopic variables as "reservoir" variables but must treat them on an equal footing.

C. Initial-charge and final-charge distributions

Now we have only to obtain the initial-charge distribution for obtaining the charge-interval distribution. Since we neglect the traversal time for tunneling, the initial-charge distribution coincides with the displaced final-charge distribution:

$$P^{\text{initial}}(Q) = P^{\text{final}}(Q + e), \tag{3.7}$$

where the final-charge distribution $P^{\text{final}}(Q)$ gives the probability density that the tunneling event occurs at charge Q. On the other hand, the final-charge distribution is related to the initial-charge distribution via $P(Q_i, Q_f)$:

$$P^{\text{final}}(Q_f) = \int_{-\frac{e}{2}}^{Q_f} P^{\text{initial}}(Q_i) P(Q_i, Q_f) dQ_i. \tag{3.8}$$

Dividing the range of integration at $D \equiv \min\left(\frac{e}{2}, CV - e\right)$, we have

$$P^{\text{final}}(Q_f) = P\left(\frac{e}{2}, Q_f\right) \int_{-\frac{e}{2}}^{D} P^{\text{initial}}(Q_i) dQ_i + \int_{D}^{Q_f} P^{\text{initial}}(Q_i) P(Q_i, Q_f) dQ_i, \tag{3.9}$$

where $P\left(\frac{e}{2}, Q_f\right)$ in the first term of the rhs is factored out because from Eq. (3.5) we have $P(Q_i, Q_f) = P\left(\frac{e}{2}, Q_f\right)$ for $Q_i < \frac{e}{2}$. Equations (3.7) and (3.9) determine the initial-charge distribution. In the following discussion, however, we will restrict ourselves to the important case of $CV < \frac{3}{2}e$ for which these equations can then be solved exactly. For $CV < \frac{3}{2}e$, the first integral on the rhs of Eq. (3.9) gives unity because of the normalization condition, while the second integral vanishes because $P^{\text{initial}}(Q_i) = 0$ for $Q_i > CV - e$. Thus we have

$$P^{\text{final}}(Q_f) = P\left(\frac{e}{2}, Q_f\right) \quad \text{for} \quad CV < \frac{3}{2}e, \tag{3.10}$$

and from Eq. (3.7) we obtain

$$P^{\text{initial}}(Q_i) = P\left(\frac{e}{2}, Q_i + e\right) \quad \text{for} \quad CV < \frac{3}{2}e. \tag{3.11}$$

It is easy to see that the initial charge distribution satisfies the following normalization condition:

$$\int_{-\frac{e}{2}}^{CV-e} P^{\text{initial}}(Q_i) dQ_i = 1. \tag{3.12}$$

Figure 8 illustrates the initial-charge and final-charge distributions for several values of the ratio $\frac{R_S}{R_T}$ with $CV = e$. All the final-charge distributions rise above $\frac{e}{2}$ because tunneling is inhibited until the accumulated charge exceeds $\frac{e}{2}$. Curve (e) with $\frac{R_S}{R_T} = 300$ is sharply distributed just above $\frac{e}{2}$. This is because the tunneling lifetime ($\sim CR_T$) is much shorter than the time needed to recharge the junction ($\sim CR_S$). Thus tunneling events are expected to occur very regularly. As the ratio $\frac{R_S}{R_T}$ decreases, the tunneling lifetime becomes relatively larger, and hence the distribution becomes broader. Thus tunneling events are expected to occur increasingly at random. From this figure only, however, we cannot see how regularly

tunneling events occur for each curve. For this purpose, it is necessary to obtain the time-interval distribution $P_{s11}(\tau)$. The time interval τ between two consecutive tunneling events is related to the corresponding initial charge Q_i and final charge Q_f via a simple circuit equation:

$$\tau = -CR_S \ln \frac{CV - Q_f}{CV - Q_i}. \tag{3.13}$$

Each combination of Q_i and Q_f that gives the same time interval τ through this equation contributes to $P_{s11}(\tau)$ with weight function $P_{s11}(Q_i, Q_f)$. Thus

$$P_{s11}(\tau) = \int_{-\frac{e}{2}}^{CV-e} dQ_i \int_{\frac{e}{2}}^{CV} dQ_f P_{s11}(Q_i, Q_f)\, \delta\left(\tau + CR_S \ln \frac{CV - Q_f}{CV - Q_i}\right). \tag{3.14}$$

The integration with respect to Q_f can be carried out by noting that

$$\delta\left(\tau + CR_S \ln \frac{CV - Q_f}{CV - Q_i}\right) = \frac{CV - Q_f}{CR_S}\, \delta\left[Q_f - Q_i e^{-\frac{\tau}{CR_S}} - CV\left(1 - e^{-\frac{\tau}{CR_S}}\right)\right], \tag{3.15}$$

giving

$$\begin{aligned} P_{s11}(\tau) = {} & \theta(CV - e - B) \int_B^{CV-e} dQ_i\, P_{s11}\left[Q_i, Q_i e^{-\frac{\tau}{CR_S}} + CV\left(1 - e^{-\frac{\tau}{CR_S}}\right)\right] \\ & \times \frac{CV - Q_i}{CR_S} e^{-\frac{\tau}{CR_S}}, \end{aligned} \tag{3.16}$$

where

$$B \equiv \max\left[-\frac{e}{2}, CV - e^{\frac{\tau}{CR_S}}\left(CV - \frac{e}{2}\right)\right]. \tag{3.17}$$

The lower bound of integration B comes from the following consideration. If we specify τ and Q_i, then Q_f is uniquely determined from Eq. (3.13). On the other hand, Q_f cannot take values below $\frac{e}{2}$ because of Coulomb blockade. To meet this requirement, the integration range for Q_i must have a lower bound which yields B. To put it another way, the tunnel junction cannot be charged up to $\frac{e}{2}$ during a time τ if the initial charge is below B.

Equation (3.16) gives a general expression of the time-interval distribution in terms of the charge-interval distribution. For $CV < \frac{3}{2}e$, we can obtain the analytic expression of $P_{s11}(Q_i, Q_f)$. In fact, from Eqs. (3.2) and (3.11), we obtain

$$P_{s11}(Q_i, Q_f) = P\left(\frac{e}{2}, Q_i + e\right) P\left(\frac{e}{2}, Q_f\right) \quad \text{for} \quad CV < \frac{3}{2}e, \tag{3.18}$$

where $P(Q_i, Q_f) = P\left(\frac{e}{2}, Q_f\right)$ since $Q_i < \frac{e}{2}$ for $CV < \frac{3}{2}e$. Substituting Eq. (3.18) into Eq. (3.16) we can calculate the time-interval distribution as a function of junction and circuit parameters.

Figure 9 shows time-interval distributions for various values of the ratio $\frac{R_S}{R_T}$ with fixed bias voltage $V = \frac{e}{C}$, where the time axis is normalized by CR_S. Curve (a) with $\frac{R_S}{R_T} = 300$ is sharply distributed around 1.2 CR_S. This curve clearly demonstrates regular SET oscillations in the time domain. We observe that this curve has a finite width. It will be shown in Sec. 4 that this width *never* goes to zero but only reaches the quantum-originated nonzero value even in the ideal limit of the constant-current operation. As the ratio $\frac{R_S}{R_T}$ decreases, the distribution becomes less and less localized, and the regularity of SET events becomes worse. Thus we have demonstrated the crossover from random to Coulomb-regulated SET oscillations in the *time domain* as the external source changes from a voltage source to a current source.

3.3. Tunneling lifetime

In general, the dynamics of mesoscopic normal tunnel junctions are characterized by the power spectrum of voltage across the junction. However, since in our case at most one electron tunnels at one time, tunneling characteristics can be more directly described by the probability distribution of time intervals between consecutive tunneling events, i.e., the probability distribution of tunneling lifetimes. Suppose that a tunneling event occurred at time t_i and the first subsequent tunneling event occurred at time t_f. Then the lifetime is defined as

$$\tau(Q_i, Q_f) \equiv t_f - t_i, \tag{3.19}$$

where Q_i and Q_f represent the charge just *after* the first tunneling event occurred and the charge just *before* the second tunneling event will occur, respectively (see Fig. 7). From Eq. (3.13) we have

$$\tau(Q_i, Q_f) = CR_S \ln \frac{CV - Q_i}{CV - Q_f}. \tag{3.20}$$

The average lifetime $\overline{\tau}$ is, in general, given by

$$\overline{\tau} = \int_{-\frac{e}{2}}^{CV-e} dQ_i \int_{\frac{e}{2}}^{CV} dQ_f \; \tau(Q_i, Q_f) P_{s11}(Q_i, Q_f). \tag{3.21}$$

For $CV < \frac{3}{2}e$, substituting Eqs. (3.18) and (3.20) into the rhs of Eq. (3.21) yields

$$\overline{\tau} = CR_S \int_{\frac{e}{2}}^{CV} dQ \ln \frac{CV + e - Q}{CV - Q} P\left(\frac{e}{2}, Q\right). \tag{3.22}$$

This is an exact expression of the average lifetime as a function of junction and circuit parameters, where an explicit expression of $P\left(\frac{e}{2}, Q\right)$ is given by Eq. (3.5). To proceed further with calculation, let us expand logarithmic terms in terms of parameters $p \equiv \frac{e}{2CV}$ and $q \equiv \frac{Q-\frac{e}{2}}{CV}$

$$\ln \frac{CV+e-Q}{CV-Q} = \ln \frac{CV+\frac{e}{2}}{CV-\frac{e}{2}} + \ln\left(1-\frac{q}{1+p}\right) - \ln\left(1-\frac{q}{1-p}\right)$$
$$= \ln \frac{CV+\frac{e}{2}}{CV-\frac{e}{2}} + \frac{2p}{1-p^2}q + \frac{2p}{(1-p^2)^2}q^2 + \frac{2p+\frac{2}{3}p^3}{(1-p^2)^3}q^3 + \frac{2p+2p^3}{(1-p^2)^4}q^4 + O(q^5). \quad (3.23)$$

This expansion can be justified because moments of $q(\overline{q}, \overline{q^2}, \text{etc.})$ rapidly converge to zero as the ratio $\frac{R_S}{R_T}$ becomes larger (see Appendix B). Substituting Eq. (3.23) into Eq. (3.22) yields

$$\overline{\tau} = CR_S\left[\ln \frac{CV+\frac{e}{2}}{CV-\frac{e}{2}} + \frac{2p}{1-p^2}\overline{q} + \frac{2p}{(1-p^2)^2}\overline{q^2} + \frac{2p+\frac{2}{3}p^3}{(1-p^2)^3}\overline{q^3} + \frac{2p+2p^3}{(1-p^2)^4}\overline{q^4} + O(q^5)\right], \quad (3.24)$$

where moments of q are given in Appendix A.

Fluctuation properties of SET oscillations can be characterized using the variance of lifetimes defined by

$$\overline{(\Delta\tau)^2} \equiv \overline{\tau^2} - \overline{\tau}^2, \quad (3.25)$$

where the mean square of dwell times, $\overline{\tau^2}$, is given by

$$\overline{\tau^2} = \int_{-\frac{e}{2}}^{CV-e} dQ_i \int_{\frac{e}{2}}^{CV} dQ_f \; \tau^2(Q_i, Q_f) P_{s11}(Q_i, Q_f). \quad (3.26)$$

For $CV < \frac{3}{2}e$, substituting Eq. (3.18) into Eq. (3.26) yields

$$\overline{\tau^2} = (CR_S)^2 \int_{\frac{e}{2}}^{CV} dQ \int_{\frac{e}{2}}^{CV} dQ' \left[\ln\left(\frac{CV+e-Q}{CV-Q'}\right)\right]^2 P\left(\frac{e}{2}, Q\right) P\left(\frac{e}{2}, Q'\right). \quad (3.27)$$

Expanding the logarithmic term in terms of p, q, and $q' \equiv \frac{Q'-\frac{e}{2}}{CV}$, we obtain a perturbation expansion for $\overline{\tau^2}$ which, combined with Eq. (3.24), yields

$$\overline{(\Delta\tau)^2} = 2(CR_s)^2\left[\frac{1+p^2}{(1-p^2)^2}(\overline{q^2} - \overline{q}^2) + \frac{1+3p^2}{(1-p^2)^3}(\overline{q^3} - \overline{q}\,\overline{q^2}) + O(q^4)\right]. \quad (3.28)$$

These formulas will be used for later discussion.

3.4. Current-voltage characteristics

The probability distribution of charge across the junction, $P(Q)$, is given by

$$P(Q) = \frac{\overline{\tau}(Q)}{\overline{\tau}}, \quad (3.29)$$

where $\overline{\tau}$ is the average lifetime given by Eq. (3.22) and $\overline{\tau}(Q)$ is defined such that $\overline{\tau}(Q)dQ$ gives the average time during which the charge on the junction lies between Q and $Q+dQ$:

$$\overline{\tau}(Q)dQ = \int_{-\frac{e}{2}}^{CV-e} dQ_i \int_{\frac{e}{2}}^{CV} dQ_f \; \tau(Q, Q+dQ) P_{s11}(Q_i, Q_f) \times \theta(Q-Q_i)\theta(Q_f-Q). \tag{3.30}$$

Substituting Eqs. (3.22) and (3.30) into Eq. (3.29) yields

$$P(Q) = \frac{CR_S}{CV-Q} \frac{\int_{-\frac{e}{2}}^{CV-e} dQ_i \int_{\frac{e}{2}}^{CV} dQ_f \; P_{s11}(Q_i, Q_f)\theta(Q-Q_i)\theta(Q_f-Q)}{\int_{-\frac{e}{2}}^{CV-e} dQ_i \int_{\frac{e}{2}}^{CV} dQ_f \; \tau(Q_i, Q_f) P_{s11}(Q_i, Q_f)}. \tag{3.31}$$

It can be verified that $P(Q)$ given by Eq. (3.31) satisfies the following normalization condition

$$\int_{-\frac{e}{2}}^{CV} P(Q)dQ = 1. \tag{3.32}$$

For $CV < \frac{3}{2}e$, substituting Eq. (3.18) into the numerator of Eq. (3.31) yields

$$P(Q) = \begin{cases} \frac{1}{\overline{\tau}} \frac{CR_S}{CV-Q} \left[1 - \exp\left(-\int_{\frac{e}{2}}^{Q+e} \frac{\tau(q)}{\tau(q)} dq\right)\right] & \text{for } -\frac{e}{2} < Q < CV - e, \\ \frac{1}{\overline{\tau}} \frac{CR_S}{CV-Q} & \text{for } CV - e < Q < \frac{e}{2}, \\ \frac{1}{\overline{\tau}} \frac{CR_S}{CV-Q} \exp\left[-\int_{\frac{e}{2}}^{Q} \frac{\tau(q)}{\tau(q)} dq\right] & \text{for } \frac{e}{2} < Q < CV. \end{cases} \tag{3.33}$$

Equation (3.33) gives an exact expression of the charge distribution across the junction under an arbitrary bias condition. The voltage distribution $P(V)$ across the junction is uniquely related to the charge distribution $P(Q)$ by $P(V) = P(Q)\frac{dQ}{dV} = CP(Q)$. Figure 10 illustrates the charge distributions for several values of the ratio $\frac{R_S}{R_T}$ with fixed bias voltage $V = \frac{e}{C}$. Curve (a) with $\frac{R_S}{R_T} = 300$ rapidly rises above $-\frac{e}{2}$ and rapidly falls above $\frac{e}{2}$. This reflects the fact that SET oscillations occur very regularly. As the ratio $\frac{R_S}{R_T}$ decreases, both rises and falls become less and less sharp, and finally the distribution diverges at $Q = CV$. At this point the bias condition effectively changes from a constant-current to a constant-voltage operation.

The expected value of the junction charge is given by

$$\overline{Q} = \int_{-\frac{e}{2}}^{CV} QP(Q)dQ. \tag{3.34}$$

Substituting Eq. (3.33) into the rhs of Eq. (3.34) yields

$$\overline{Q} = CV - CR_S\frac{e}{\overline{\tau}}, \tag{3.35}$$

and hence

$$\overline{V} = V - R_S \frac{e}{\overline{\tau}}. \tag{3.36}$$

This equation has a simple physical interpretation. The quantity

$$\overline{I} = \frac{e}{\overline{\tau}} \tag{3.37}$$

is the average current through the barrier. On average, the same amount of current should flow in the external circuit and this causes a voltage drop of $R_S\overline{I}$ in the source resistance. Equation (3.36) therefore means that the average voltage across the junction is equal to the source voltage V minus the voltage drop in the source resistance (Kirchhoff's second law). It is interesting to note that Kirchhoff's second law, exemplified by Eq. (3.36), does not hold for a single tunneling event. This is because tunneling events occur quantum-mechanically and hence any classical equation is recovered, if ever, in the sense of the ensemble average (Ehrenfest's law).

3.5. Relationship to the conventional master-equation approach

Let us discuss the relationship of the probability-density-function approach to the conventional master-equation approach. The master-equation approach deals with the probability distribution $P(Q,t)$ of the junction charge Q at time t which is assumed to obey the stochastic master equation (2.9). The probability-density-function approach considers the case at zero temperature. In this case, backward tunneling plays no role because, once the accumulated charge becomes larger than $-\frac{e}{2}$, it will never enter the region $Q < -\frac{e}{2}$ in which backward tunneling is possible. Thus the probability-density-function approach gives results that are equivalent to those obtained by the conventional master-equation approach. In particular, Eq. (3.33) gives a stationary solution of Eq. (2.9) at zero temperature.

4. Standard quantum limit and shot noise of mesoscopic tunneling current

SET oscillations may be utilized for various applications in quantum metrology, supersensitive electrometry and digital microelectronics.[1] The singnal-to-noise ratio of single-electron devices is ultimately determined by the degree of randomness of SET events. It is therefore of great significance to determine the maximum signal-to-noise ratio of SET events. The ultimate signal-to-noise ratio is not determined by thermal or current fluctuations but is determined by quantum fluctuations inherent in SET oscillations. This section demonstrates the existence of the fundamental quantum limit of SET oscillations which we shall refer to as the *standard quantum limit*, and shows a crossover from the random shot noise to the Coulomb-regulated standard quantum limit as the bias condition is continuously changed from a constant-voltage to a constant-current operation.

4.1. Degree of randomness of SET events

To quantitatively evaluate quantum noise of SET oscillations, let us introduce a quantity that we shall refer to as the *degree of randomness of SET events*. It is natural to define this as the standard deviation of dwell times divided by their average value:

$$\sigma \equiv \frac{\sqrt{\overline{(\Delta\tau)^2}}}{\overline{\tau}}, \tag{4.1}$$

where $\overline{(\Delta\tau)^2} \equiv \overline{\tau^2} - \overline{\tau}^2$. A Poisson random-point process gives $\sigma = 1$, while a completely regular-point process gives $\sigma = 0$. In general, the smaller the value of σ, the more regularly SET events occur. The main concern here is to find the functional form of σ under an arbitrary bias condition.

4.2. Constant-voltage operation — shot noise

Under constant-voltage operation where $\frac{R_S}{R_T} \ll 1$, one cannot apply the perturbation technique but must use exact expressions (3.22) and (3.27). A straightforward calculation yields

the mean lifetime as

$$\overline{\tau} = CR_T \left[\frac{e}{CV - \frac{\varepsilon}{2}} + \frac{R_S}{R_T} \ln \frac{e}{CV - \frac{\varepsilon}{2}} \right]. \tag{4.2}$$

Here the first term on the rhs of this equation is proportional to CR_T as is the case for a macroscopic tunnel junction under the constant-voltage operation, but the first term differs from the macroscopic formula by prefactor $\frac{CV}{CV - \frac{\varepsilon}{2}}$. This reflects the fact that Coulomb blockade still works under almost constant-voltage operation as a *dc offset* and that it prolongs the lifetime by the same prefactor. On the other hand, the second term gives the first-order correction due to a nonvanishing source (or shunt) resistance R_S.

The variance of tunneling lifetimes can be calculated, from Eq. (3.27), to give

$$\overline{(\Delta\tau)^2} = \left(CR_T \frac{e}{CV - \frac{\varepsilon}{2}} \right)^2. \tag{4.3}$$

Hence we obtain the expression of the degree of randomness under almost constant-voltage operation as

$$\sigma = \frac{1}{1 + \frac{R_S}{R_T} \frac{CV - \frac{\varepsilon}{2}}{e} \ln \frac{e}{CV - \frac{\varepsilon}{2}}}. \tag{4.4}$$

Thus we find that SET events are indeed regulated (i.e., $\sigma < 1$) by the nonvanishing source resistance and Coulomb blockade. As the ratio $\frac{R_S}{R_T}$ approaches zero, however, SET events tend to occur completely at random (i.e., $\sigma = 1$), although Coulomb blockade still serves to prolong the average lifetime by prefactor $\frac{CV}{CV - \frac{\varepsilon}{2}}$ (see Eq. (4.2)). This can be understood as follows. When the source resistance is negligibly small, the tunneling rate is almost always pinned at $r(CV) = \frac{CV - \frac{\varepsilon}{2}}{eR_T C}$ whose offset $\frac{\varepsilon}{2}$ explains the prefactor. At the same time, since the tunneling rate is constant, SET events obey a Poisson random-point process; hence we obtain $\sigma = 1$. This is a microscopic version of the Schottky formula which we encounter in macroscopic junctions:

$$S_I(\omega) = \frac{e}{2\pi} \overline{I}, \tag{4.5}$$

where $S_I(\omega)$ is the power spectrum of tunneling current and $\overline{I}$ is the average tunneling current $\overline{I} = er(CV)$.

4.3. Constant-current operation — standard quantum limit

Under the constant-current operation where $\frac{R_S}{R_T} \gg 1$ and $\frac{V}{R_S} = I_{dc}$, Eq. (3.24) reduces to

$$\overline{\tau} = \frac{e}{I_{dc}} \left[1 + \sqrt{\frac{\pi}{2} \frac{R_T}{R_S} \frac{e}{CV} \left(1 - \frac{e}{2CV} \right)} \right]. \tag{4.6}$$

The first term on the rhs of this equation gives the celebrated relation

$$\overline{\tau} = \frac{1}{f}, \tag{4.7}$$

where $f = \frac{e}{I_{dc}}$ is the characteristic frequency of SET oscillations. The second term represents the first-order correction to Eq. (4.7) due to a finite tunnel resistance R_T.

The degree of randomness of SET events is obtained by substituting Eqs. (3.24) and (3.28) into Eq. (4.1):

$$\sigma = 2 \frac{\sqrt{\frac{1+p^2}{(1-p^2)^2} \left(\overline{q^2} - \overline{q}^2 \right) + \frac{1+3p^2}{(1-p^2)^3} \left(\overline{q^3} - \overline{q}\,\overline{q^2} \right)}}{\ln \frac{1+p}{1-p} + \frac{2p}{1-p^2} \overline{q} + \frac{2p}{(1-p^2)^2} \overline{q^2}} + O(q^2). \tag{4.8}$$

The minimum degree of randomness of SET events can be achieved under the constant-current operation. Taking the limit $R_S \to \infty$ and $V \to \infty$ with $\frac{V}{R_S} = I_{dc}$ of Eq. (4.8) yields

$$\sigma_{SQL} = \sqrt{(4 - \pi) \frac{R_T C I_{dc}}{e}}, \tag{4.9}$$

where SQL stands for the standard quantum limit. It is remarkable that even under the ideal constant-current operation, the degree of randomness never goes to zero but only reaches the nonzero value given by Eq. (4.9). This apparently contradicts the result obtained by the conventional stochastic method using computer simulation, where SET oscillations appear to have a zero linewidth and the stochastic nature of tunneling events emerges as a broad background noise (or "pedestral"). To check the consistency of our probability-density-function approach with the conventional approach, we carried out a computer simulation according to the conventional approach for the constant current of $I_{dc} = 0.1 \frac{e}{R_T C}$. It turns out that the computer simulation also gives a finite degree of randomness

$$\sigma_{\text{computer simulation}} = 0.2925, \tag{4.10}$$

while our theoretical result (4.9) gives

$$\sigma_{SQL} = 0.2929, \tag{4.11}$$

in perfect agreement with (4.10) within the accuracy of the computer simulation. We have performed similar simulations for several values of the current $\left(\leq 0.1\frac{e}{R_T C}\right)$ and confirmed perfect consistency between the two approaches.

It is true that the residual degree of randomness in the time domain does not necessarily lead to a finite linewidth in the voltage spectrum of SET oscillations, but, nonetheless, it is problematic that SET oscillations do have zero linewidth because the residual degree of randomness means fluctuations in the tunneling lifetime which usually implies a finite linewidth. The apparent zero linewidth may be due to the coarseness of time steps taken in computer simulation. A more detailed examination, however, will be needed to reach a definite conclusion about the linewidth problem.

4.4. Crossover from shot noise to standard quantum limit

We have shown that statistics of SET events feature shot noise under the constant-voltage operation. We have also found that the degree of randomness never goes to zero but only reaches the standard quantum limit. Now let us examine the crossover from shot noise to standard quantum limit by numerically calculating exact formulas (3.22) and (3.27).

Figure 11 shows the normalized degree of randomness as a function of ratio $\frac{R_S}{R_T}$ for several values of the product CV. Here σ_{SQL} is calculated from Eq. (4.9) in which I_{dc} is set equal to the average current $\frac{e}{\bar{\tau}}$ corresponding to each ratio $\frac{R_S}{R_T}$. We find that in all curves the degree of randomness approaches the standard quantum limit as the source is continuously changed from a voltage to a current source. The physical origin of this limit will be discussed in the following section.

5. Origin of the standard quantum limit

In the previous section we saw that the degree of randomness of SET events never goes to zero but only reaches the standard quantum limit under the ideal constant-current operation. We note that this residual degree of randomness does not originate from current or from thermal fluctuations. So where does the limit come from? In fact, the standard quantum limit emerges complementarily from energy uncertainty through the time-energy uncertainty principle that is inherent in quantum-mechanical tunneling. Now let us discuss this issue within the framework of semiclassical theory.

5.1. Time uncertainty — fluctuations in tunneling lifetimes

The standard quantum limit originates from the uncertainty with respect to the time when an electron starts to tunnel. According to quantum mechanics, what we can predict is the probability of an electron tunneling at a particular time. To exactly predict whether or not it actually tunnels at that time is impossible, in principle. Hence comes the time uncertainty. In the semiclassical approximation where the traversal time for tunneling is disregarded, time uncertainty is attributed solely to fluctuations in tunneling lifetimes. Under the ideal constant-current operation where $R_S \to \infty$ and $V \to \infty$ with $\frac{V}{R_S} = I_{dc}$, we obtain from Eq. (4.9)

$$\Delta t \equiv \sqrt{\overline{(\Delta\tau)^2}} = \sqrt{(4-\pi)\frac{eR_TC}{I_{dc}}}. \tag{5.1}$$

This can be understood as follows. If the bias current I_{dc} is small, then the average value of tunneling lifetimes becomes long, and so does their standard deviation. On the other hand, if the time constant CR_T is large, then the average tunneling lifetime becomes long, and so does its standard deviation.

5.2. Energy uncertainty — fluctuations in Coulomb energy

In normal metal tunnel junctions, there is no energy due to phase coherence. Furthermore, we do not incorporate the process of thermalization in our model. Fluctuations in Coulomb energy are, therefore, the only source of energy uncertainty. The average Coulomb energy is

given from Eq. (C.9) by

$$\overline{E}_{\text{Coulomb}} = \frac{\overline{Q^2}}{2C} = \frac{CV^2}{2}\left[1 - \frac{R_S}{V}\frac{e}{\overline{\tau}}(1+\overline{q})\right]. \tag{5.2}$$

Under almost constant-current operation, Eq. (3.24) reduces to

$$\overline{\tau} = e\frac{R_S}{V}\left[1 + \overline{q} + \overline{q^2} + \overline{q^3} + \overline{q^4} + \cdots\right]. \tag{5.3}$$

Substituting Eq. (5.3) into Eq. (5.2) yields

$$\overline{E}_{\text{Coulomb}} = \frac{CV^2}{2}\frac{\overline{q^2} + \overline{q^3} + \overline{q^4} + \cdots}{1 + \overline{q} + \overline{q^2} + \overline{q^3} + \overline{q^4} + \cdots}. \tag{5.4}$$

The mean square of Coulomb energy is given from Eq. (C.11) by

$$\begin{aligned}\overline{E^2}_{\text{Coulomb}} &= \overline{\left(\frac{Q^2}{2C}\right)^2} \\ &= \left(\frac{CV^2}{2}\right)^2\left\{1 - \frac{R_S}{V}\frac{e}{\overline{\tau}}\left[1 + \frac{1}{12}\left(\frac{e}{CV}\right)^2 + \left(1 + \frac{1}{4}\left(\frac{e}{CV}\right)^2\right)\overline{q} + \overline{q^2} + \overline{q^3}\right]\right\}.\end{aligned} \tag{5.5}$$

Under almost constant-current operation, Eq. (5.5) reduces to

$$\overline{E^2}_{\text{Coulomb}} = \left(\frac{CV^2}{2}\right)^2\frac{\overline{q^4} + \overline{q^5} + \cdots}{1 + \overline{q} + \overline{q^2} + \overline{q^3} + \overline{q^4} + \cdots}. \tag{5.6}$$

From Eqs. (5.4) and (5.6) we obtain

$$\Delta E \equiv \sqrt{\overline{E^2}_{\text{Coulomb}} - \left(\overline{E}_{\text{Coulomb}}\right)^2} = eR_T I_{dc}. \tag{5.7}$$

5.3. Time-energy uncertainty relationship in tunneling

From Eqs. (5.1) and (5.7) we obtain

$$\Delta t \Delta E = e^2 R_T \sqrt{(4-\pi)\frac{R_T C I_{dc}}{e}} = e^2 R_T \sigma_{SQL}, \tag{5.8}$$

where σ_{SQL} is given by Eq. (4.9). Since we adopt a semiclassical model which assumes that

$$R_T \geq R_Q = \frac{h}{e^2}, \tag{5.9}$$

we obtain

$$\Delta t \Delta E \geq h\sigma_{SQL}. \tag{5.10}$$

Thus we find that there is a trade-off relationship between fluctuations in tunneling lifetimes and fluctuations in Coulomb energy. Such a trade-off relationship can be intuitively understood as follows. First, we recall that in the semiclassical approximation time and energy uncertainties are attributed solely to fluctuations in tunneling lifetimes and in Coulomb energy, respectively. When the tunnel resistance R_T is very large compared to the resistance quantum R_Q, an electron is almost always localized on one or the other side of the barrier. Thus the energy uncertainty is very small. However, the tunneling lifetime then becomes very large and so does the time uncertainty. On the other hand, when the tunnel resistance is very small (but still larger than R_Q), the tunneling rate is very large and therefore the time uncertainty is very small. However, is this case, an electron cannot be localized on either side of the barrier and therefore fluctuations in Coulomb energy become very large.

Relationship (5.10) is different from the familiar time-energy uncertainty relationship[40] in that the lower bound includes σ_{SQL}. This reflects the fact that the state of the junction is determined not only by the junction characteristic itself but also by the bias condition. Although relationship (5.9) is derived under the constant-current operation, it is straightforward to show that the rhs gives the lowest bound for an arbitrary bias condition because the degree of randomness takes the minimum value for the constant-current operation. Thus we have obtained a special form of the time-energy uncertainty relationship that is unique to single-electron tunneling by Coulomb blockade.

5.4. Breakdown of semiclassical theory of Coulomb blockade

The derivation of the time-energy uncertainty relationship shows a critical point where the semiclassical theory of Coulomb blockade manifestly breaks down. The essential assumption in deriving this relationship is $R_T \geq R_Q$. However, it is possible to fabricate a tunnel junction such that the opposite inequality, $R_T < R_Q$, holds. In this case, the time-energy uncertainty relationship apparently breaks down. Such a conclusion clearly contradicts the principle of quantum mechanics and must be attributed to a semiclassical assumption that becomes invalid for $R_T < R_Q$. As the tunnel resistance becomes smaller and smaller, the time uncertainty also becomes smaller. However, fluctuations in the Coulomb energy of a single electron due

to delocalization of the electron wavefunction cannot be larger than $e^2/2C$. To relax this restriction, we must take into account quantum fluctuations associated with the traversal time for tunneling, and thermal and electrical relaxation processes, both of which are neglected in the semiclassical theory.

6. Infrared divergence in single-electron tunneling

This section develops a finite-temperature theory of small tunnel junctions that accounts for both Coulomb suppression and zero-bias anomaly in tunneling conductance under the influence of many-body final-state interaction in normal electrodes. It will be shown that a sudden change in the localized Coulomb potential due to single-electron tunneling excites an infinite number of electrons and holes near the Fermi surface. Such an infrared catastrophe leads to a power-law anomaly in the density of final states that are available for tunneling. In particular, a general formula for the frequency-dependent tunneling rate is obtained whose anomalous power exponent is determined consistently with the Friedel sum rule.

A mathematical technique to cope with infrared catastrophe caused by a sudden change in the localized potential was developed by Nozières and Dominicis[42] in the x-ray problem, and it was extended to finite temperatures by Yuval and Anderson[43] in the Kondo problem. We apply the same technique to the problem of many-body final-state interaction in tunneling. We reproduce their method wherever necessary to avoid the need for constant reference to their papers.

6.1. Effects of the "Fermi-surface" environment on tunneling

Suppose that a normal tunnel junction with capacitance C is initially in a thermal equilibrium state. According to the orthodox theory of Coulomb blockade, the forward tunneling rate is given by Eq. (2.1). The key assumption in deriving this equation is that the state immediately after tunneling is again in a thermal equilibrium state. To put it another way, the orthodox theory assumes that the transient behavior between the two equilibrium states before and after tunneling can be neglected. This assumption may be justified for large junctions because the perturbation brought about by a single tunneling event is usually negligible. For small tunnel junctions with capacitance smaller than 1 fF, however, a sudden voltage change $\frac{e}{C}$ due to a single tunneling event is of the order of meV, and therefore the ensuing electrical relaxation significantly renormalizes the density of final states that are available for tunneling.

The electrical relaxation consists of two stages with different time scales. In the first stage, the surface-charge formation is completed during the time scale of the inverse plasma frequency

(screening process). Following this stage, the electronic configuration undergoes fine rearrangement by low-energy electron-hole pairs excited near the Fermi surface by the screened Coulomb potential. The crucial observation here is that the number of excited electron-hole pairs becomes *infinite* no matter how weak the screened Coulomb potential is (infrared catastrophe), and that the tunneling process will not have been completed until the excess charge brought by electron tunneling and the phase shifts of conduction electrons induced by it become balanced by the Friedel sum rule. When the vacuum field fluctuations associated with such final-state interaction become appreciable compared to the single-electron charging energy, the effect of Coulomb blockade will be greatly modified.

This is the physical picture of what we shall refer to as the "Fermi-surface" environment. We nonperturbatively incorporate the second stage into the theory based on the microscopic Hamiltonian because infrared-divergent creation of electron-hole pairs makes an ordinary perturbation technique invalid.[44] The "Fermi-surface" environment is responsible for the electrical relaxation in the second state. On the other hand, the excited electronic states are coupled with the thermal reservoir, which is in the long run responsible for the thermal relaxation. We also incorporate this process into the theory using real-time Green's functions.

6.2. Formulation of the problem

A. Model Hamiltonian

As described above, the orthodox theory of Coulomb blockade neglects a transient response to a sudden potential change due to tunneling. In contrast, we take into account the second stage of the electrical relaxation and the associated thermal relaxation. Since this is basically the rearrangement of the electronic configuration by the screened Coulomb potential, it can be incorporated into the theory by introducing time-dependent scattering terms

$$\sum_{k \neq k} V^L_{kk'}(t) c^\dagger_k c_{k'} \quad \text{and} \quad \sum_{q \neq q'} V^R_{qq'}(t) c^\dagger_q c_{q'}$$

into the model Hamiltonian. Throughout this paper it is understood that k, k' refer to the left electrode and that q, q', p refer to the right electrode. $V^L_{kk'}$ and $V^R_{qq'}$ are set equal to zero before a tunneling event occurs, and are switched on suddenly when a tunneling event occurs. We

assume that they are constant afterwards. Suppose that a tunneling event occurs from the right to the left (see Fig. 12). $V^L_{kk'}$ (or $V^R_{qq'}$) then describes the scattering by the screened Coulomb potential on the left (or right) electrode. Since they are suddenly switched on upon tunneling, we assume that they are zero before the tunneling event occurs and constant afterwards.

These scattering terms rearrange conduction electrons, performing fine adjustment to a new electrical equilibrium state. Our model Hamiltonian is therefore given by

$$H = H_L + H_R + H_T + H_C, \tag{6.1}$$

$$H_L = \sum_k \varepsilon_k c^\dagger_k c_k + \sum_{k \neq k'} V^L_{kk'}(t) c^\dagger_k c_{k'}, \tag{6.2}$$

$$H_R = \sum_q \varepsilon_q c^\dagger_q c_q + \sum_{q \neq q'} V^R_{qq'}(t) c^\dagger_q c_{q'}, \tag{6.3}$$

$$H_T = \sum_{k,q} \left(T_{kq} c^\dagger_k c_q + T_{qk} c^\dagger_q c_k \right), \tag{6.4}$$

$$H_C = \frac{Q^2}{2C}, \quad Q = -\frac{e}{2}(N_L - N_R) + \text{const.} = e\left(N_R - \frac{N}{2}\right) + \text{const.}, \tag{6.5}$$

where N_L (or N_R) is the number operator of electrons in the left (or right) electrode, and $N \equiv N_L + N_R$. We note that Eqs. (6.1)–(6.5) are the standard Hamiltonian of a normal tunnel junction except that Eqs. (6.2) and (6.3) include the scattering terms. These many-body interactions will play an essential role in the electrical relaxation process and lead to renormalization of the density of final states available for tunneling which is responsible for the zero-bias anomaly in the tunneling conductance.

B. Response function of the tunneling Hamiltonian

According to the linear response theory, the tunneling characteristic is determined by the response function of the tunneling Hamiltonian[45]

$$iR(t - t') = \langle 0 | T \{ H_T(t) H_T(t') \} | 0 \rangle, \tag{6.6}$$

where t' and t denote the times of two consecutive tunneling events. Here $|0\rangle$ denotes the state of the junction just before the first tunneling event occurs, and the T product orders operators

from right to left in ascending time order and adds a factor $(-1)^P$, where P is the number of interchanges of fermion operators from the original given order. Substituting Eq. (6.4) into this equation yields

$$\begin{aligned} iR(t-t') = \; & 2 \quad |T|^2 \sum_{k,k'} \langle 0|T\left\{c_k(t)c_{k'}^\dagger(t')\right\}|0\rangle u_k u_{k'} \\ & \times \sum_{qq'} \langle 0|T\left\{c_{q'}(t')c_q^\dagger(t)\right\}|0\rangle u_q u_{q'} + \text{c.c.}, \end{aligned} \tag{6.7}$$

where c.c. means complex conjugation and we have used the fact that the Coulomb part of the Hamiltonian, H_C, can be expressed solely in terms of the operators of the right electrode, which allows the decoupling of the total amplitude into two parts. In deriving Eq. (6.7) we have also assumed that the matrix elements of the tunneling Hamiltonian are separable (i.e. $T_{kk'} = T u_k u_{k'}$). We use the same notation T for the magnitude of the tunneling matrix elements as for the time-ordering operator because there is no fear of confusion.

We define transient Green's functions $\mathcal{G}^L_{kk'}$ and $\mathcal{G}^R_{qq'}$ which describe the transient response of conduction electrons in the left and right electrodes to the sudden potential change due to tunneling.

$$i\mathcal{G}^L_{kk'}(t-t') = \langle 0|T\left\{c_k(t)c_{k'}^\dagger(t')\right\}|0\rangle, \tag{6.8}$$

$$i\mathcal{G}^R_{qq'}(t-t') = \langle 0|T\left\{c_q(t)c_{q'}^\dagger(t')\right\}|0\rangle, \tag{6.9}$$

Since in Eq. (6.7) transient Green's functions appear in forms summed over momentum variables, it is convenient to define

$$\mathcal{G}^L(t-t') = \sum_{k,k'} \mathcal{G}^L_{k,k'}(t-t')u_k u_{k'}, \tag{6.10}$$

$$\mathcal{G}^R(t-t') = \sum_{q,q'} \mathcal{G}^R_{q,q'}(t-t')u_q u_{q'}. \tag{6.11}$$

Substituting Eqs. (6.10) and (6.11) into Eq. (6.7), we obtain

$$R(t-t') = 2i|T|^2 \mathcal{G}^R(t-t')^* \mathcal{G}^L(t-t') + \text{c.c.}, \tag{6.12}$$

where the asterisk denotes complex conjugation. The problem thus reduces to obtaining transient Green's functions $\mathcal{G}^R$ and $\mathcal{G}^L$ under the influence of the sudden potential change due to tunneling.

C. Temperature Green's functions

In treating systems at finite temperatures, it will be most convenient to consider the grand canonical ensemble because the number of electrons in each electrode fluctuates in time. The single-particle temperature Green's function is defined as

$$G^R_{qp}(\tau) \equiv -\langle T_\tau \left\{ c_q(\tau) c_p^\dagger(0) \right\} \rangle, \tag{6.13}$$

where the angle brackets $\langle \cdots \rangle$ denote the statistical average over a certain restricted ensemble and T_τ denotes the time-ordering operator for the imaginary time. The operators $c_q(\tau)$ and $c_q^\dagger(\tau)$ are defined by

$$c_q(\tau) = e^{K\tau/\hbar} c_q \, e^{-K\tau/\hbar}, \quad c_q^\dagger(\tau) = e^{K\tau/\hbar} c_q^\dagger \, e^{-K\tau/\hbar}, \tag{6.14}$$

where

$$K = H - \mu_L H_L - \mu_R H_R. \tag{6.15}$$

Here μ_L and μ_R are the electrochemical potentials of the left and right electrodes. The Heisenberg equation of motion for $c_q(\tau)$ is given from Eq. (6.14) by

$$\hbar \frac{d}{d\tau} c_q(\tau) = [K, c_q(\tau)]. \tag{6.16}$$

Substituting Eq. (6.15) into Eq. (6.16) yields

$$\hbar \frac{d}{d\tau} c_q(\tau) = -(\varepsilon_q - \mu_R) c_q(\tau) - \sum_{q'} V^R_{qq'} c_{q'}(\tau) - \frac{e}{c} c_q(\tau) \left(Q(\tau) - \frac{e}{2} \right). \tag{6.17}$$

Hence, the equation of motion for $G^R_{qp}(\tau)$ becomes

$$\frac{d}{d\tau} G^R_{qp}(\tau) = -\delta(\tau)\delta_{qp} - \hbar^{-1} \left(\varepsilon_q - \mu_R + \frac{e}{c}(Q - \frac{e}{2}) \right) G^R_{qp}(\tau) - \hbar^{-1} \sum_{q'} V_{qq'} G^R_{q'p}(\tau). \tag{6.18}$$

In deriving Eq. (6.18) the following decoupling approximation is made

$$\langle T\tau \left\{ c_q(\tau) \left(Q(\tau) - \frac{e}{2} \right) c_q^\dagger(0) \right\} \rangle = \left(Q - \frac{e}{2} \right) \langle T\tau \left\{ c_q(\tau) c_q^\dagger(0) \right\} \rangle. \tag{6.19}$$

The temperature Green's function and the delta function can be expanded in Fourier series

$$G^R_{qp}(\tau) = (\beta\hbar)^{-1} \sum_n G^R_{qp}(\omega_n) e^{-i\omega_n \tau}, \tag{6.20}$$

$$\delta(\tau) = (\beta\hbar)^{-1}\sum_n e^{-i\omega_n\tau}, \tag{6.21}$$

where $\omega_n = \frac{(2n+1)\pi}{\beta\hbar}$ gives the Matsubara frequencies for fermions and $\beta \equiv \frac{1}{k_B T}$. Substituting Eqs. (6.20) and (6.21) into Eq. (6.18), we obtain

$$G^R(\omega_n) = \frac{G_0^R(\omega_n)}{1-\hbar^{-1}VG_0^R(\omega_n)}, \tag{6.22}$$

where

$$G_0^R(\omega_n) = \sum_q G_0^R(q,\omega_n)u_q^2, \tag{6.23}$$

and

$$G_0^R(q,\omega_n) = \frac{\hbar}{i\hbar\omega_n - (\varepsilon_q - \mu_R) - \frac{e}{c}(Q-\frac{e}{2})}, \tag{6.24}$$

where we have assumed that the scattering terms are separable (i.e. $V_{kk'}^L = V^L u_k u_{k'}$, etc.). This assumption means that we consider only the S-wave scattering. The real-time Green's function $\bar{G}_0^R$ can be obtained by performing analytic continuation of Eq. (6.24) to real times. Thus we obtain

$$\begin{aligned}\bar{G}_0^R(q,\omega) = \quad & (1-f_F(\varepsilon_q-\mu_R+\Delta))\frac{\hbar}{\hbar\omega-(\varepsilon_q-\mu_R)-\Delta+i\eta} \\ & +f_F(\varepsilon_q-\mu_R+\Delta)\frac{\hbar}{\hbar\omega-(\varepsilon_q-\mu_R)-\Delta-i\eta},\end{aligned} \tag{6.25}$$

where η is positive and infinitesimal, and $\Delta = \frac{e}{C}\left(Q-\frac{e}{2}\right)$ is the difference in the electrostatic potential before and after tunneling. Equation (6.25) shows that the effect of the potential change due to tunneling is incorporated into the real-time Green's function as a shift in energy by an amount of Δ. This energy shift and the electrochemical potential are erased, however, if we inversely Fourier-transform Eq. (6.25):

$$\bar{G}_0^R(t) = -\frac{\frac{\pi\rho_0^R}{\beta}}{\sinh\frac{\pi t}{\beta\hbar}}, \tag{6.26}$$

where ρ_0^R is the density of energy states which is assumed to be constant for all energies.

6.3. Transient Green's functions at finite temperatures

A. Asymptotic expressions of conduction-electron Green's functions

The real-time Green's function (6.26) is correct for times that are long compared to the inverse bandwidth of conduction electrons, but it becomes invalid for shorter times. We assume

that the Green's function at shorter times can be approximated as the delta function. If the strength of the delta function is set equal to $\pi\rho_0\hbar\tan\theta$, then we have

$$\bar{G}_0^R(t) = -\frac{\pi\rho_0^R}{\beta}\left[P\left(\frac{1}{\sinh\frac{\pi t}{\beta\hbar}}\right)+\pi\tan\theta\delta\left(\sinh\frac{\pi t}{\beta\hbar}\right)\right]e^{-i(\mu_R+\Delta)t/\hbar}. \tag{6.27}$$

Fourier transformation of this equation yields

$$\begin{aligned}\bar{G}_0^R(\omega) &= \int_{-\infty}^{\infty}dt\bar{G}_0^R(t)e^{i\omega t}\\ &= -\pi\rho_0^R\hbar\left[i\tanh\frac{\beta}{2}(\hbar\omega-\mu_R-\Delta)+\tan\theta\right].\end{aligned} \tag{6.28}$$

Substituting Eq. (6.28) into Eq. (6.22) yields

$$\bar{G}^R(\omega) = -\pi\rho_0^R\hbar\frac{i\tanh\frac{\beta}{2}(\hbar\omega-\mu_R-\Delta)+\tan\theta-\pi g_0^R\left(\tanh^2\frac{\beta}{2}(\hbar\omega-\mu_R-\Delta)+\tan^2\theta\right)}{1-2\pi g_0^R\tan\theta+(\pi g_0^R)^2\left(\tanh^2\frac{\beta}{2}(\hbar\omega-\mu_R-\Delta)+\tan^2\theta\right)}, \tag{6.29}$$

where $g_0^R\equiv\rho_0^RV^R$. We can choose real parameters α^R and θ' such that the rhs of Eq. (6.29) may be rewritten as

$$\bar{G}^R(\omega) = -\alpha^R\pi\rho_0^R\hbar\left[i\tanh\frac{\beta}{2}(\hbar\omega-\mu_R-\Delta)+\tan\theta'\right]. \tag{6.30}$$

By comparing Eqs. (6.29) and (6.30), we obtain

$$\alpha^R = \left[1-2\pi g_0^R\tan\theta+(\pi g_0^R)^2\left(\tanh^2\frac{\beta}{2}(\hbar\omega-\mu_R-\Delta)+\tan^2\theta\right)\right]^{-1}, \tag{6.31}$$

and

$$\tan\theta' = \tan\theta-\pi g_0^R\left(\tanh^2\frac{\beta}{2}(\hbar\omega-\mu_R-\Delta)+\tan^2\theta\right). \tag{6.32}$$

It is convenient to define the renormalized coupling constant g^R and the phase shift δ_R of conduction electrons at the Fermi surface by

$$g^R = g_0^R\frac{\tanh^2\frac{\beta}{2}(\hbar\omega-\mu_R-\Delta)+\tan^2\theta}{1+\tan^2\theta}, \tag{6.33}$$

and

$$\delta_R = \theta-\theta', \tag{6.34}$$

respectively. It can be shown that the phase shift and the coupling constant are related by

$$\tan\delta_R = \frac{\pi g^R}{1-\pi g^R \tan\theta}. \tag{6.35}$$

The α^R in Eq. (6.31) can be expressed in terms of the renormalized coupling constant g^R as

$$\alpha^R = \left[1 - 2\pi g^R \tan\theta + \frac{(\pi g^R)^2}{\cos^2\theta}\right]^{-1}. \tag{6.36}$$

This quantity may also be written in terms of the phase shift as

$$\alpha^R = \left(\frac{\sin\delta_R}{\pi g}\right)^2 = \frac{\cos^2(\theta-\delta_R)}{\cos^2\theta} = \frac{1}{\pi}\frac{d\delta_R}{dg}. \tag{6.37}$$

Substituting Eqs. (6.34) and (6.37) into Eq. (6.30) yields

$$\bar{G}^R(\omega) = -\pi\rho_0^R\hbar\frac{\cos^2(\theta-\delta_R)}{\cos^2\theta}\left[i\tanh\frac{\beta}{2}(\hbar\omega-\mu_R-\Delta)+\tan(\theta-\delta_R)\right]. \tag{6.38}$$

Inverse Fourier transformation of this equation finally gives

$$\bar{G}^R(t) = -\frac{\pi\rho_o^R}{\beta}\frac{\cos^2(\theta-\delta_R)}{\cos^2\theta}\left[P\left(\frac{1}{\sinh\frac{\pi t}{\beta\hbar}}\right)+\pi\tan(\theta-\delta_R)\delta\left(\sinh\frac{\pi t}{\beta\hbar}\right)\right]e^{-i(\mu_R+\Delta)t/\hbar}. \tag{6.39}$$

This is the desired asymptotic expression of the conduction-electron Green's function on the right electrode after the electrical relaxation is completed. It describes a new equilibrium state of the right electrode after tunneling. The corresponding Green's function for the left electrode can be obtained by replacing the quantities of the right electrode by those of the left one. Now we will derive the transient Green's function of conduction electrons after tunneling which eventually reaches the state described by Eq. (6.39).

B. Transient Green's function for the total system

The transient Green's function of the left electrode describes the propagation of a tunneling electron, the collective propagation of the localized potential, and the associated many-body interaction such as vertex corrections and self-energy renormalizations. A typical diagram is shown in Fig. 13 (a). We assume that the localized potential is time-independent. The propagation of the localized potential then contributes to the transient Green's function only as an exponential factor. The dotted line in Fig. 13 (a), which represents the propagation of

the localized potential, can therefore be eliminated to give Fig. 13 (b) in which the distinction between self-energy renormalizations and vertex corrections disappears. Thus the transient Green's function is given by the product of a dressed propagator of a tunneling electron for the left electrode (or that of a hole created by it for the right electrode) and the contributions of loops:

$$i\mathcal{G}^R(t) = L^R(t)e^{C^R(t)}. \tag{6.40}$$

$$i\mathcal{G}^L(t) = L^L(t)e^{C^L(t)}. \tag{6.41}$$

We note that the many-body graph in Fig. 13 (a) is reduced to a time-dependent one-body graph and that the time-dependence enters only as boundary conditions. Since the self-energy renormalizations and vertex corrections become single loops, their contributions can be summed up using the linked-cluster theorem.[42] This observation greatly facilitates the exact treatment of the transient Green's function which would otherwise be impossible to calculate without recourse to approximation schemes.

C. Transient Green's function for conduction electrons

Suppose that one electron tunnels through the barrier from right to left at time t. We are then interested in the transient Green's function $\varphi^R_{qq'}(\tau,\tau';t_0,t)$ which describes the fine adjustment of conduction electrons to the new equilibrium state described by Eq. (6.39). We assume that no tunneling events will occur until the new equilibrium state is reached. Since the "free" propagator after the first tunneling event occurs is given by $\bar{G}^R(t)$ in Eq. (6.39), the transient Green's function must obey the following Dyson equation

$$\varphi^R_{qq'}(\tau,\tau';\,t_0,t) = \bar{G}^R_{qq'}(\tau-\tau') + i\int_{t_0}^{t} dt'' \sum_{pp'} \bar{G}^R_{qp}(\tau-\tau'')V^R_{pp'}\varphi^R_{p'q'}(\tau'',\tau';t_0,t). \tag{6.42}$$

This equation can be solved to give[43]

$$\varphi^R(\tau,\tau';\,t_0,t) = \bar{G}^R(\tau-\tau')\left[\frac{\sinh\frac{\pi}{\beta\hbar}(t-\tau')\sinh\frac{\pi}{\beta\hbar}(\tau-t_0)}{\sinh\frac{\pi}{\beta\hbar}(t-\tau)\sinh\frac{\pi}{\beta\hbar}(\tau'-t_0)}\right]^{\frac{\epsilon_R}{\pi}}. \tag{6.43}$$

This Green's function gives a transient response to a sudden potential change due to tunneling. The effect of the transient response is simply expressed by an algebraic factor. We note that, as time progresses, the transient Green's function tends to become the new equilibrium state described by Eq. (6.39).

D. Dressed propagators of a tunneling electron and a hole created by it

The propagator of a tunneling electron and that of a hole created by it are renormalized by the static vertex correction (see Fig. 13 (b)). The dressed propagator of the hole is given by setting $\tau \to t$ and $\tau' \to t_0$ in Eq. (6.43).

$$L^R(t) = \underset{\tau \overrightarrow{\to} t_0}{\mathrm{Im}} \; -\varphi^R(\tau, \tau'; t_0, t) = \frac{\alpha^R \frac{\pi}{\beta\hbar} \rho_0^R \hbar}{\sinh \frac{\pi}{\beta\hbar}(t - t_0)} \left[\frac{\sinh \frac{\pi}{\beta\hbar}(t - t_0)}{\sinh \frac{\pi}{\beta\hbar} \tau_{\mathrm{cut}}^R} \right]^{2\frac{\delta_R}{\pi}}, \tag{6.44}$$

where τ_{cut}^R, whose order of magnitude is the inverse plasma frequency, is introduced to avoid the spurious divergence of the algebraic factor. This divergence is caused by taking the asymptotic expression (6.39) for the free propagator, and it should disappear in a more exact treatment. The dressed propagator of the tunneling electron can be obtained by replacing the quantities of the right electrode by those of the left one.

E. Contribution of closed loops

The contribution of closed loops is to carry information about vacuum field fluctuations induced by a sudden potential change due to tunneling. It follows from the fluctuation-dissipation theorem that the closed loops bear a close relationship to the decay of the transient Green's function of conduction electrons. The decay is controlled by the algebraic factor, which is decomposed into unity and a smaller factor:

$$\frac{\sinh \frac{\pi}{\beta\hbar}(t - \tau') \sinh \frac{\pi}{\beta\hbar}(\tau - t_0)}{\sinh \frac{\pi}{\beta\hbar}(t - \tau) \sinh \frac{\pi}{\beta\hbar}(\tau' - t_0)} = 1 + \frac{\sinh \frac{\pi}{\beta\hbar}(t - t_0) \sinh \frac{\pi}{\beta\hbar}(\tau - \tau')}{\sinh \frac{\pi}{\beta\hbar}(t - \tau) \sinh \frac{\pi}{\beta\hbar}(\tau' - t_0)}. \tag{6.45}$$

Using this we may expand φ^R near $\tau = \tau'$ as

$$\varphi^R(\tau, \tau'; t_0, t) = \bar{G}_0^R(\tau - \tau') - \alpha^R \frac{\pi}{\beta\hbar} \rho_0^R \frac{\delta_R}{\pi} \left(\coth \frac{\pi}{\beta\hbar}(\tau' - t_0) + \coth \frac{\pi}{\beta\hbar}(t - \tau) \right). \tag{6.46}$$

The contribution of closed loops C^R satisfies[42]

$$g\frac{\partial}{\partial g}C^R(t-t_0) = -V\int_{t_0}^{t}\varphi^R(\tau,\tau;t_0,t)d\tau. \tag{6.47}$$

Substituting Eq. (6.46) into Eq. (6.47) yields

$$\frac{\partial}{\partial g}C^R(t-t_0) = -2\alpha^R\frac{\delta_R}{\pi}\ln\left(\frac{\sinh\frac{\pi}{\beta\hbar}(t-t_0)}{\sinh\frac{\pi}{\beta\hbar}\tau^R_{\rm cut}}\right). \tag{6.48}$$

This equation combined with Eq. (6.37) finally yields

$$C^R(t-t_0) = -\left(\frac{\delta_R}{\pi}\right)^2\ln\left(\frac{\sinh\frac{\pi}{\beta\hbar}(t-t_0)}{\sinh\frac{\pi}{\beta\hbar}\tau^R_{\rm cut}}\right). \tag{6.49}$$

Thus we obtain the transient Green's functions of the right and left electrodes as

$$\mathcal{G}^R(t) = -i\frac{\pi}{\beta\hbar}\frac{\alpha^R\rho_0^R\hbar}{\sinh\frac{\pi}{\beta\hbar}t}\left[\frac{\sinh\frac{\pi}{\beta\hbar}t}{\sinh\frac{\pi}{\beta\hbar}\tau^R}\right]^{\frac{\delta_R}{\pi}-\left(\frac{\delta_R}{\pi}\right)^2}e^{-i(\mu^R+\Delta)t/\hbar}, \tag{6.50}$$

$$\mathcal{G}^L(t) = -i\frac{\pi}{\beta\hbar}\frac{\alpha^L\rho_0^L\hbar}{\sinh\frac{\pi}{\beta\hbar}t}\left[\frac{\sinh\frac{\pi}{\beta\hbar}t}{\sinh\frac{\pi}{\beta\hbar}\tau^R}\right]^{\frac{\delta_L}{\pi}-\left(\frac{\delta_L}{\pi}\right)^2}e^{-i\mu^Lt/\hbar}. \tag{6.51}$$

6.4. Renormalized response function of the tunneling Hamiltonian

A. General formula

The response function of the tunneling Hamiltonian is given by Eq. (6.12). For the time being we consider only the forward tunneling to make our logic clear. Then we have

$$iR(t) = 2|T|^2\mathcal{G}^R(t)^*\mathcal{G}^L(t). \tag{6.52}$$

Substituting Eqs. (6.50) and (6.51) into Eq. (6.52) yields

$$\begin{aligned} iR(t) = {} & 2|T|^2\left(\frac{\pi}{\beta}\right)^2\frac{\alpha^R\rho_0^R}{\sinh\frac{\pi}{\beta\hbar}\tau^R_{\rm cut}}\frac{\alpha^L\rho_0^L}{\sinh\frac{\pi}{\beta\hbar}\tau^L_{\rm out}}\left[\frac{\sinh\frac{\pi}{\beta\hbar}t}{\sinh\frac{\pi}{\beta\hbar}\tau^R_{\rm cut}}\right]^{2\frac{\delta_R}{\pi}-\left(\frac{\delta_R}{\pi}\right)^2-1} \\ & \times\left[\frac{\sinh\frac{\pi}{\beta\hbar}t}{\sinh\frac{\pi}{\beta\hbar}\tau^L_{\rm cut}}\right]^{2\frac{\delta_L}{\pi}-\left(\frac{\delta_L}{\pi}\right)^2-1}e^{t\{(\mu^R-\mu^L)+\Delta\}t/\hbar}\theta(t). \end{aligned} \tag{6.53}$$

We note that V^L and V^R are equal in magnitude but opposite in sign because conduction electrons in each electrode are scattered by mirror charges on opposite sides of the barrier. The phase shifts δ_L and δ_R are therefore equal in magnitude but opposite in sign.

$$\delta_R = -\delta_L \equiv \delta. \tag{6.54}$$

To simplify matters we assume that the electrochemical potential and the cut-off of conduction electrons are common to both electrodes

$$\mu^R = \mu^L \equiv \mu, \tag{6.55}$$

$$\tau^R_{\rm out} = \tau^L_{\rm cut} \equiv \tau. \tag{6.56}$$

Equation (6.53) then reduces to

$$R(t) = -iA(\sinh \frac{\pi}{\beta\hbar}t)^{-g-2}e^{i\Delta t/\hbar}\theta(t), \tag{6.57}$$

where

$$A = \left(\frac{\pi}{\beta}\right)^2 \frac{2\alpha^L\alpha^R\hbar}{e^2R_T}(\sinh \frac{\pi}{\beta\hbar}\tau_{\rm cut})^g, \tag{6.58}$$

and R_T is the tunnel resistance

$$R_T = \frac{\hbar}{e^2|T|^2\rho_0^L\rho_0^R}. \tag{6.59}$$

Fourier transformation of Eq. (6.57) yields (see Appendix D)

$$R(\omega) = 2i\frac{A}{\frac{\pi}{\beta\hbar}}\frac{\sin\left(iy+\frac{g}{2}\right)}{\sin\pi g}\int_0^\infty dt\frac{\cos(2yt)}{(\cosh t)^{g+2}}, \tag{6.60}$$

where $y \equiv \frac{\beta}{2\pi}(\hbar\omega + \Delta)$. The tunneling rate is given by the imaginary part of the response function. It is given by

$$\mathrm{Im}R(\omega) = \frac{A}{\frac{\pi}{\beta\hbar}}\frac{\cosh\pi y}{\cos\frac{\pi}{2}t}\int_0^\infty dt\frac{\cos(2yt)}{(\cosh t)^{g+2}}. \tag{6.61}$$

This result can be written in terms of the Beta function by using the relation

$$\int_0^\infty dt\frac{\cosh 2yt}{(\cosh t)^{2x}} = 2^{2x-2}B(x+y, x-y), \tag{6.62}$$

where $B(x,y)$ is the Beta function defined by

$$B(x,y) \equiv \int_0^1 t^{x-1}(1-t)^{y-1}dt. \tag{6.63}$$

Equation (6.61) then becomes

$$\mathrm{Im}R(\omega) = A\frac{2g}{\frac{\pi}{\beta\hbar}}\frac{\cosh \pi y}{\cos\frac{\pi}{2}g} B\left(iy+\frac{g}{2}+1, -iy+\frac{g}{2}+1\right). \tag{6.64}$$

The general frequency-dependent forward tunneling rate is thus given by

$$r(Q,\omega) = \frac{1}{\pi\hbar^2}\mathrm{Im}R(\omega) = \frac{\alpha^L\alpha^R}{e^2R_T}\frac{4g}{\beta}\ B\left(iy+\frac{g}{2}+1, -iy+\frac{g}{2}+1\right). \tag{6.65}$$

This is the main result of this section. We will examine two specific cases to check this result.

B. Reduced formula for $T = 0$

We first consider the zero-temperature limit. In this case, it is convenient to start from a gamma function representation of Eq. (6.65).

$$R(\omega) = -iA\frac{2^{g+1}}{\frac{\pi}{\beta\hbar}}\frac{\pi}{\sin\pi g}\frac{1}{\Gamma(g+2)}\frac{\Gamma\left(-iy+\frac{g}{2}+1\right)}{\Gamma\left(-iy-\frac{g}{2}\right)}. \tag{6.66}$$

As the temperature reduces to zero, the parameter y becomes infinite. Using the asymptotic expansion of the ratio

$$\frac{\Gamma(z+\alpha)}{\Gamma(z+\beta)} = z^{\alpha-\beta}\left[1+\frac{(\alpha-\beta)(\alpha+\beta-1)}{2z}+0(|z|^{-2})\right], \tag{6.67}$$

we obtain

$$R(\omega) = -\frac{\alpha^R\alpha^L\hbar^3}{e^2R_T\tau_{\mathrm{cut}}}\frac{2\pi}{\sin\pi g}\frac{e^{-i\frac{\pi}{2}g}}{\Gamma(g+2)}\left(\frac{\hbar\omega+\Delta}{\hbar/\tau_{\mathrm{cut}}}\right)^{1+g}. \tag{6.68}$$

The imaginary parts of this expression yield

$$\mathrm{Im}R(\omega) = \frac{\alpha^R\alpha^L\hbar^3}{e^2R_T\tau_{\mathrm{cut}}}\frac{\pi}{\cos\frac{\pi}{2}g}\frac{1}{\Gamma(g+2)}\left(\frac{\hbar\omega+\Delta}{\hbar/\tau_{\mathrm{cut}}}\right)^{1+g}. \tag{6.69}$$

From this result we obtain the frequency-dependent tunneling rate at zero temperature as

$$r(Q,\omega) = \frac{1}{\pi\hbar^2}\mathrm{Im}R(\omega) = \frac{\alpha^R\alpha^L}{(\hbar/\tau_{\mathrm{cut}})^g}\frac{1}{\cos\frac{\pi}{2}g}\frac{1}{\Gamma(g+2)}\frac{(\hbar\omega+\Delta)^{1+g}}{e^2R_T}. \tag{6.70}$$

This result is identical to that obtained in an earlier letter.[31]

C. Reduced formula for $g = 0$

Next, we examine the orthodox limit $g = 0$ of the general formula (6.65). Since the beta function in Eq. (6.65) assumes the form

$$B(iy+1, -iy+1) = \Gamma(1+iy, 1-iy) = \frac{\pi y}{\sinh \pi y}, \tag{6.71}$$

the imaginary part of the response function reduces to

$$\mathrm{Im}R(\omega) = \pi\hbar^2 \frac{\hbar\omega + \Delta}{e^2 R_T} \coth \frac{\hbar\omega + \Delta}{2k_B T}. \tag{6.72}$$

From this expression we obtain the frequency-dependent forward tunneling rate as

$$r(Q,\omega) = \frac{1}{\pi\hbar^2}\mathrm{Im}R(\omega) = \frac{\hbar\omega + \frac{e}{C}\left(Q - \frac{e}{2}\right)}{e^2 R_T} \frac{1}{1 - \exp\left(-\frac{1}{k_B T}\left(\hbar\omega + \frac{e}{C}\left(Q - \frac{e}{2}\right)\right)\right)}. \tag{6.73}$$

Similarly the backward tunneling rate is given by

$$l(Q,\omega) = \frac{\hbar\omega - \frac{e}{C}\left(Q + \frac{e}{2}\right)}{e^2 R_T} \frac{1}{\exp\left(\frac{1}{k_B T}\left(\hbar\omega + \frac{e}{C}\left(Q + \frac{e}{2}\right)\right)\right) - 1}. \tag{6.74}$$

These results are identical to those obtained earlier by a different method.[46][47]

6.5. Determination of anomalous power exponent

Finally, let us determine the anomalous power exponent g. It is given by the Friedel sum rule that gives a self-consistent condition between a localized excess charge and phase shifts of conduction electrons induced by it. In general, if the excess charge in units of e is Z, then it is related to the phase shifts of conduction electrons at the Fermi surface as

$$Z = \frac{2}{\pi} \Sigma_l \, (2l+1) \, \delta_l(k_F), \tag{6.75}$$

where δ_l is the phase shift of the scattered wave with angular momentum l. Since we consider only the S-wave scattering ($l = 0$) and the accumulated charge after tunneling is given by $Q_f - e$, we have

$$\frac{Q_f - e}{e} = \frac{2}{\pi}\delta \longrightarrow g = 2\left(\frac{\delta}{\pi}\right)^2 = \frac{1}{2}\left(\frac{Q_f - e}{e}\right)^2, \tag{6.76}$$

where Q_f denotes the accumulated charge just before a tunneling event occurs.

To test our prediction the bias current must be chosen very small so that the next tunneling event will never occur in the second state. In addition to the usual requirements for the observation of single-charging effects, the bias current should therefore be much smaller than 1 nanoampere; that is, we must operate SET oscillations at frequencies much lower than 1 GHz. This explains why our prediction has not been observed to date.

7. Discussion and conclusions

This paper developed two theories on micro-tunnel junctions: Sections 3 to 5 are devoted to the probability-density-function description of mesoscopic normal tunnel junctions and Section 6 considers infrared divergence in single-electron tunneling. This section summarizes and discusses the main results of the present paper.

Tunneling current in macroscopic junctions usually features shot noise known as the Schottky formula, and external dynamical variables can be eliminated as reservoir variables via the fluctuation-dissipation theorem. The underlying physics by which such a conventional picture may be justified is that tunneling events occur exclusively as a result of the wave nature of an electron and that background thermal noise is overwhelming enough to ensure thermal equilibration of the external circuit and to allow elimination of its dynamical variables via the fluctuation-dissipation theorem because then back action of tunneling events on the external circuit may well be neglected.

However, in ultrasmall tunnel junctions where the electrostatic energy of a single electron becomes comparable to or even larger than the masking thermal energy, such a conventional picture breaks down because firstly, Coulomb regularization of tunneling events becomes important and secondly, the back action of tunneling events can no longer be disregarded. We cannot resort to the linear response theory to eliminate external dynamical variables, but must to treat both the junction and external circuit on an equal footing. The probability-density-function approach to mesoscopic tunnel junctions described in this paper is developed to attack such problems analytically. We note that the key distribution (3.5) includes both junction and circuit parameters in a manner that cannot be disentangled.

The standard quantum limit is shown to originate from neither thermal nor current noise but from the time-energy uncertainty relationship that is inherent in quantum-mechanical tunneling. This limit imposes a fundamental limit on the signal-to-noise ratio of "single-electron devices" such as single-electron transistors and logic elements.[1]

Uncertainty with respect to the time when an electron starts to tunnel is based on a particle picture of an electron, but the uncertainty is shown to arise complementarily from the energy uncertainty due to delocalization of an electron wavefunction over both electrodes. Thus the

time-energy uncertainty relationship in tunneling is closely related to the wave-particle duality of an electron. We have derived a particular form of the time-energy uncertainty relationship whose lower bound includes the degree of randomness for the standard quantum limit. This again reflects the fact that we must treat both junction and external circuit on an equal footing. The essential assumption in deriving Eq. (5.10) is $R_T \geq R_Q$. However, it is possible to fabricate a tunnel junction such that the opposite inequality, $R_T < R_Q$, holds. In this case the time-energy uncertainty relationship apparently breaks down. Such a conclusion clearly contradicts the principle of quantum mechanics and must be attributed to a semiclassical assumption that becomes invalid for $R_T < R_Q$. As the tunnel resistance becomes smaller and smaller, the time uncertainty also becomes smaller. However, fluctuations in the Coulomb energy of a single electron due to delocalization of the electron wavefunction cannot be larger than $e^2/2C$. To relax this restriction, we must take into account some quantum fluctuations or the traversal time for tunneling, both of which are neglected in the semiclassical theory.

Section 6 considers the effect of the "Fermi-surface environment on tunneling. A sudden change in the localized Coulomb potential due to single-electron tunneling excites an infinite number of electrons and holes near the Fermi surface. Such an infrared-divergent shake-up is shown to renormalize the density of final states available for tunneling until a localized excess charge and phase shifts of conduction electrons induced by it become balanced by the Friedel sum rule. This situation is schematically illustrated in Fig. 14.

It is, in general, very important to take account of the effect of recoil due to the finite mass of a potential source when we consider the localized dynamic perturbation in metals.[48] In our problem, however, this effect of recoil can be neglected mainly because it is a collective potential formed from all the conduction electrons and background ions in electrodes so the excitation energy of the collective potential becomes too high ($\sim$ several eV, plasma energy) to get it recoiled. Needless to say, the plasma oscillations are very important during a very short time ($10^{-14} - 10^{-15}$ seconds—the first stage) immediately after a tunneling event occurs. For normal metal junctions, however, infrared divergent excitation of electron-hole pairs near the Fermi surface occurs on a much longer time scale (10^{-11} seconds or even longer—the second stage).

The effect of the electromagnetic environment along the transmission line and that of the

electron-hole pair creation should be regarded as complementary. Both effects result from the same tunneling Hamiltonian

$$H_T = \sum_{k,q} \left(T_{kq} e^{-i\phi} c_k^\dagger c_q + T_{kq}^* e^{i\phi} c_q^\dagger c_k \right). \tag{7.1}$$

In the previous literature[3]–[6] the former effect was discussed by calculating the correlation function of the electromagnetic phase without regard to the many-body final-state interaction of conduction electrons, while the present paper discusses the latter effect by calculating the correlation function of conduction electrons without regard to the electromagnetic phase. The former effect crosses over to the latter as the frequency of SET oscillations decreases. At the frequencies at which recent experiments on Coulomb blockade were performed, the effect of electron-hole pairs should appear as the radiative correction to the electromagnetic environment. Indeed, loop contributions calculated in the present paper are nothing but the radiative corrections. To unify both pictures we must treat both sources of dissipation on an equal footing. A unified theory of single-electron tunneling, in which both environments are taken into account, can be constructed by incorporating the electromagnetic field into our theory via the gauge-invariant replacement of momentum operators P by the canonical correspondents $P - \frac{e}{c}A$. Such an extension, however, remains as future work.

8. Appendices

A. Moments of normalized final charge $\overline{q^n}$

Let us evaluate the quantity

$$f_n \equiv \int_{\frac{e}{2}}^{CV} Q^n \exp\left[-\int_{\frac{e}{2}}^{Q} \frac{r(q)}{i(q)}\right] dQ \tag{A.1}$$

when $k_B T \ll \frac{e^2}{2C}$ and no noise current is generated in the source resistance. Then substituting the expressions

$$r(q) = \frac{q - \frac{e}{2}}{e R_T C} \theta\left(q - \frac{e}{2}\right) \tag{A.2}$$

and

$$i(q) = \frac{CV - q}{C R_S} \tag{A.3}$$

into Eq. (A.1) yields

$$f_n = \int_{\frac{e}{2}}^{CV} Q^n \left(\frac{CV - Q}{CV - \frac{e}{2}}\right)^{\frac{1}{e}\frac{R_S}{R_T}\left(CV - \frac{e}{2}\right)} \exp\left[\frac{1}{e}\frac{R_S}{R_T}\left(Q - \frac{e}{2}\right)\right] dQ \tag{A.4}$$

If we change the integration variable to $t = \frac{1}{e}\frac{R_S}{R_T}(CV - Q)$ and set $a \equiv \frac{1}{e}\frac{R_T}{R_S}$, $b \equiv CV$, $c \equiv \frac{\exp(d)}{d^d}$, and $d \equiv \frac{1}{e}\frac{R_S}{R_T}\left(CV - \frac{e}{2}\right) = \frac{b - \frac{e}{2}}{a}$, we obtain

$$f_n = ac \int_0^d (b - at)^n \, t^d \, \exp(-t) dt. \tag{A.5}$$

From this we see that the rhs of this equation can be expressed in terms of the incomplete gamma function defined by

$$\gamma(a, x) \equiv \int_0^x t^{a-1} \exp(-t) dt, \quad Re\ a > 0. \tag{A.6}$$

Expanding $(b - at)^n$ yields

$$f_0 = ac\gamma(d + 1, d), \tag{A.7}$$

$$f_1 = a\left[ad + \left(\frac{e}{2} - a\right) c\gamma(d + 1, d)\right], \tag{A.8}$$

$$f_2 = a\left[2ad\left(\frac{e}{2} - a\right) + \left(\left(\frac{e}{2} - a\right)^2 + a^2(d + 1)\right) c\gamma(d + 1, d)\right], \tag{A.9}$$

and

$$f_3 = a\left(3ad\left(\frac{e}{2} - a\right)^2 + a^3 d(2d + 3) + \left[\left(\frac{e}{2} - a\right)^3 + a^2(d + 1)\left(\frac{3}{2}e - 5a\right)\right] c\gamma(d + 1, d)\right), \tag{A.10}$$

where the following identity is used:[49]

$$\gamma(a+1,x) = a\gamma(a,x) - x^a e^{-x}. \tag{A.11}$$

Let us next evaluate the following quantities:

$$\overline{Q_f^n} \equiv \int_{\frac{e}{2}}^{CV} Q^n \; P\left(\frac{e}{2}, Q\right) dQ, \tag{A.12}$$

With the observation that

$$P\left(\frac{e}{2}, Q\right) = -\frac{d}{dQ} \exp\left(-\int_{\frac{e}{2}}^{Q} \frac{r(q)}{i(q)} dq\right), \tag{A.13}$$

we integrate the rhs of Eq. (A.12) by parts, obtaining

$$\overline{Q_f^n} \;=\; \left(\frac{e}{2}\right)^n + n f_{n-1}. \tag{A.14}$$

Moments of q are related to those of Q_f by

$$\overline{q^n} = \frac{\overline{\left(Q_f - \frac{e}{2}\right)^n}}{(CV)^n}. \tag{A.15}$$

Substituting Eq. (A.14) into Eq. (A.14) and using Eqs. (A.7)-(A.10) yields

$$\overline{q} = \frac{a}{b} c\gamma(d+1,d), \tag{A.16}$$

$$\overline{q^2} = 2\left(\frac{a}{b}\right)^2 [d - c\gamma(d+1,d)], \tag{A.17}$$

$$\overline{q^3} = 3\left(\frac{a}{b}\right)^3 [-2d + (d+2)c\gamma(d+1,d)], \tag{A.18}$$

and

$$\overline{q^4} = 4\left(\frac{a}{b}\right)^4 [2d(d+3) - (5d+6)c\gamma(d+1,d)]. \tag{A.19}$$

B. Asymptotic expressions of $\overline{q^n}$

(i) $\frac{R_S}{R_T} \gg 1 \longrightarrow d = \frac{R_S}{R_T}(\frac{CV}{e} - \frac{1}{2}) \gg 1$:

In this case we can make use of the following asymptotic expansion[49]

$$\gamma(d+1,d) = \sqrt{\frac{\pi}{2}} d^{d+\frac{1}{2}} \exp(-d) \left(1 - \frac{2}{3}\sqrt{\frac{2}{\pi d}} + \frac{1}{12d} + \cdots\right) \left(d \gg 1, |\arg d| < \frac{\pi}{2}\right). \tag{B.1}$$

Keeping only the first-order terms we obtain

$$\overline{q} = \left(\frac{\pi}{2}\frac{R_T}{R_S}\frac{e}{CV}\left(1-\frac{e}{2CV}\right)\right)^{\frac{1}{2}}, \tag{B.2}$$

$$\overline{q^2} = 2\frac{R_T}{R_S}\frac{e}{CV}\left(1-\frac{e}{2CV}\right), \tag{B.3}$$

$$\overline{q^3} = 3\left(\frac{\pi}{2}\right)^{\frac{1}{2}}\left(\frac{R_T}{R_S}\frac{e}{CV}\left(1-\frac{e}{2CV}\right)\right)^{\frac{3}{2}}, \tag{B.4}$$

and

$$\overline{q^4} = 8\left(\frac{R_T}{R_S}\frac{e}{CV}\left(1-\frac{e}{2CV}\right)\right)^{2}. \tag{B.5}$$

Thus we find that moments of q rapidly converge to zero as the ratio $\frac{R_S}{R_T}$ becomes larger.

(ii) $CV = \frac{e}{2}(1+\epsilon)$, $\epsilon \ll 1 \longrightarrow d = \frac{R_S}{R_T}(\frac{CV}{e} - \frac{1}{2}) \ll 1$:

In this case we can make use of the following asymptotic expansion[49]

$$\gamma(a,x) = x^a \exp(-x)\sum_{n=0}^{\infty}\frac{(a-1)!}{(a+n)!}x^n \ (a \ll 1). \tag{B.6}$$

Expanding the rhs of this equation and re-ordering in powers of d, we have

$$c\gamma(a,x) = d - \frac{d^2}{2} + \frac{5}{12}d^3 - \frac{5}{36}d^4 \ldots. \tag{B.7}$$

Substituting this expansion into the rhs of Eqs. (A.16)-(A.19), we obtain

$$\overline{q^n} = \left(\frac{e}{CV}\frac{R_T}{R_S}d\right)^n + O(d^{n+1}), \ (n = 1,2,3,4,\ldots). \tag{B.8}$$

C. Moments of charge $\overline{Q^n}$

It has been shown[24] that the charge distribution $P(Q)$ across the junction is given by

$$P(Q) = \begin{cases} \frac{1}{\overline{\tau}}\frac{CR_S}{CV-Q}\left[1-\exp\left(-\int_{\frac{e}{2}}^{Q+e}\frac{\tau(q)}{1(q)}dq\right)\right] & \text{for } -\frac{e}{2} < Q < CV - e, \\ \frac{1}{\overline{\tau}}\frac{CR_S}{CV-Q} & \text{for } CV - e < Q < \frac{e}{2}, \\ \frac{1}{\overline{\tau}}\frac{CR_S}{CV-Q}\exp\left(-\int_{\frac{e}{2}}^{Q}\frac{\tau(q)}{1(q)}dq\right) & \text{for } \frac{e}{2} < Q < CV. \end{cases} \tag{C.1}$$

Here $\overline{\tau}$ is given by Eq. (2.8). Let us calculate moments of charge Q for this distribution.

First let us verify that this distribution satisfies the normalization condition

$$\int_{-\frac{e}{2}}^{CV} P(Q)dQ = 1. \tag{C.2}$$

Substituting Eq. (C.1) into the lhs of Eq. (C.2) yields

$$\begin{aligned} \text{lhs} &= \frac{CR_S}{\overline{\tau}} \left\{ \int_{-\frac{e}{2}}^{CV-e} \frac{1}{CV-Q} \left(1 - f(Q+e)\right) dQ + \int_{CV-e}^{\frac{e}{2}} \frac{dQ}{CV-Q} + \int_{\frac{e}{2}}^{CV} \frac{1}{CV-Q} f(Q) dQ \right\} \\ &= \frac{CR_S}{\overline{\tau}} \left\{ \ln \frac{CV+\frac{e}{2}}{CV-\frac{e}{2}} + \int_{\frac{e}{2}}^{CV} \left(\frac{1}{CV-Q} - \frac{1}{CV+eQ} \right) f(Q) dQ \right\}, \end{aligned} \tag{C.3}$$

where

$$f(Q) \equiv \exp\left(- \int_{\frac{e}{2}}^{Q} \frac{r(q)}{i(q)} dq \right), \tag{C.4}$$

and $i(q) \equiv \frac{CV-q}{CR_S}$ is the injection rate of current into the junction when the accumulated charge is q. Integrating the last two terms in Eq. (C.3) by parts and using the relationship

$$P\left(\frac{e}{2}, Q\right) = -\frac{d}{dQ} f(Q), \tag{C.5}$$

we obtain

$$\int_{-\frac{e}{2}}^{CV} P(Q) dQ = \frac{1}{\overline{\tau}} \int_{\frac{e}{2}}^{CV} dQ CR_S \ln \frac{CV+e-Q}{CV-Q} P\left(\frac{e}{2}, Q\right). \tag{C.6}$$

From Eq. (2.8) we find that the rhs of this equation gives unity.

The first moment of charge is defined by

$$\overline{Q} = \int_{-\frac{e}{2}}^{CV} Q P(Q) dQ. \tag{C.7}$$

Substituting Eq. (C.1) and $Q = CV - (CV - Q)$ into (C.7) and using (C.2)

$$\overline{Q} = CV \left[1 - \frac{R_S}{V} \frac{e}{\overline{\tau}} \right]. \tag{C.8}$$

Calculation of higher-order moments can be done in a similar way. The next three moments are given by

$$\overline{Q^2} = (CV)^2 \left[1 - \frac{R_S}{V} \frac{e}{\overline{\tau}} (1 + \overline{q}) \right], \tag{C.9}$$

$$\overline{Q^3} = (CV)^3 \left[1 - \frac{R_S}{V} \frac{e}{\overline{\tau}} \left(1 + \frac{1}{12} \left(\frac{e}{CV} \right)^2 + \overline{q} + \overline{q^2} \right) \right], \tag{C.10}$$

and

$$\overline{Q^4} = (CV)^4 \left\{ 1 - \frac{R_S}{V} \frac{e}{\overline{\tau}} \left[1 + \frac{1}{12} \left(\frac{e}{CV} \right)^2 + \left(1 + \frac{1}{4} \left(\frac{e}{CV} \right)^2 \right) \overline{q} + \overline{q^2} + \overline{q^3} \right] \right\}. \tag{C.11}$$

D. Self-consistent treatment of divergent integrals

In calculating the response function, we used the following equation.

$$\int_0^\infty dt\ e^{i\mu t}(\sinh\gamma t)^\nu = \frac{1}{2^{\nu+1}\gamma}B\left(-\frac{i\mu}{2\gamma}-\frac{\nu}{2},\nu+1\right) = \frac{1}{2^{\nu+1}\gamma}\frac{\Gamma\left(-\frac{i\mu}{2\gamma}-\frac{\nu}{2}\right)\Gamma(\nu+1)}{\Gamma\left(-\frac{i\mu}{2\gamma}+\frac{\nu}{2}+1\right)}. \quad \text{(D.1)}$$

The lhs integral converges only if $\nu > -1$. Nevertheless, we applied Eq. (D.1) beyond this limit, i.e., for $\nu = -g-2$. In this Appendix we show that such extension may be justified on physical grounds. We first consider the case at zero temperature to make our logic clear. In this case Eq. (D.1) reduces to a much simpler form,

$$\int_0^\infty dt\ e^{i\mu t}\, t^\nu = \left(\frac{i}{\mu}\right)^{\nu+1}\Gamma(\nu+1). \quad \text{(D.2)}$$

Let us integrate a complex function $e^{-z}z^\nu$ along the contour shown in Fig. 15. Since the function has no singularities inside the contour, we have

$$\oint dz\ e^{-z}z^\nu = 0. \quad \text{(D.3)}$$

Since $\mathrm{Re}z > 0$ along the large arc C_4, Jordan's lemma shows that the contributions of contour C_4 vanish, and we are left with the integrals along C_1, C_2 and C_3. They are given by

$$\int_{C_1} dz\ e^{-z}z^\nu = -\left(\frac{\mu}{i}\right)^{\nu+1}\int_{\frac{\varepsilon}{\omega}}^\infty dt\ e^{i\mu t}\, t^\nu, \quad \text{(D.4)}$$

$$\int_{C_2} dz\ e^{-z}z^\nu = \frac{\varepsilon^{\nu+1}}{\nu+1}\left(1-e^{i\frac{3}{2}(\nu+1)\pi}\right), \quad \text{(D.5)}$$

$$\int_{C_3} dz\ e^{-z}z^\nu = \int_\varepsilon^\infty e^{-t}\, t^\nu\, dt \equiv \Gamma_\varepsilon(\nu+1), \quad \text{(D.6)}$$

where the function $\Gamma_\varepsilon(\nu+1)$ is defined by the last equality. Thus we have

$$\int_{\frac{\varepsilon}{\omega}}^\infty dt\ e^{i\omega t}\, t^\nu = \left(\frac{i}{\mu}\right)^{\nu+1}\left[\Gamma_\varepsilon(\nu+1)+\frac{\varepsilon^{\nu+1}}{\nu+1}\left(1-e^{i\frac{3}{2}\pi(\nu+1)}\right)\right]. \quad \text{(D.7)}$$

From this equation we find that Eq. (D.2) holds for $\nu > -1$. The first term on the rhs still diverges for $\nu < -1$ as ε approaches zero from positive values. To subtract the divergent part from Γ_ε, we consider the integral of $e^{-z}z^\nu$ along the contour C shown in Fig. 16. A similar calculation shows that

$$\Gamma_\varepsilon(\nu+1) = \frac{1}{1-e^{2\pi i\nu}}\int_C e^{-z}\, z^\nu\, dz - \frac{\varepsilon^{\nu+1}}{\nu+1}. \quad \text{(D.8)}$$

The first term on the rhs is an integral representation of the gamma function which applies not merely for $\nu > -1$ but also for $\nu < -1$ ($\nu \neq$ negative integer)

$$\Gamma^C(\nu+1) = \frac{1}{1-e^{2\pi i\nu}} \int_C e^{-z} z^\nu \, dz \quad (\nu \neq \text{negative integer}). \tag{D.9}$$

Here the superscript C is attached to emphasize the specified contour. Substituting Eqs. (D.8) and (D.9) into Eq. (D.7) yields

$$\int_{\frac{\varepsilon}{\mu}}^{\infty} dt \; e^{i\mu t} \, t^\nu = \left(\frac{i}{\mu}\right)^{\nu+1} \left[\Gamma^c(\nu+1) + i\frac{\varepsilon^{\nu+1}}{\nu+1} e^{i\frac{3}{2}\pi\nu}\right]. \tag{D.10}$$

This expression successfully separates a divergent term from a convergent one. Equation (D.10) clearly shows the divergent part comes from an integration over a range of small t or equivalently from high frequencies. Such an ultraviolet catastrophe must be healed by a finite bandwidth of conduction electrons. The remaining first part $\Gamma^C(\nu+1)$ gives a finite contribution which carries the relevant information on infrared catastrophe.

The analysis at finite temperatures proceeds in a manner similar to the zero-temperature case. We therefore write only the result of our analysis.

$$\int_{\frac{\varepsilon}{\mu}}^{\infty} dt \; e^{i\mu t} (\sinh \gamma t)^\nu = \frac{1}{2^{\nu+1}\gamma} \frac{\Gamma\left(-\frac{i\mu}{2\gamma} - \frac{\nu}{2}\right)\Gamma(\nu+1)}{\Gamma\left(-\frac{i\mu}{2\gamma} + \frac{\nu}{2} + 1\right)} - \frac{\gamma^\nu \varepsilon^{\nu+1}}{\nu+1} e^{2\pi i\nu}.$$

The rhs can be expressed in terms of the Beta function as

$$\int_{\frac{\varepsilon}{\mu}}^{\infty} dt \; e^{i\mu t} (\sinh \gamma t)^\nu = \frac{1}{2^{\nu+1}\gamma} B\left(-\frac{i\mu}{2\gamma} - \frac{\nu}{2}, \nu+1\right) - \frac{\gamma^\nu \varepsilon^{\nu+1}}{\nu+1} e^{2\pi i\nu}.$$

Thus we find that the extension of Eq. (D.1) to $\nu < -1$ implies the subtraction of an ultraviolet-divergent part from the integral which has no relevance to the problem we are concerned with.

References

[1] For reviews, see

K. K. Likharev, IBM J. Res. Dev. **32**, 144 (1988).

D. V. Averin and K. K. Likharev, "Single-Electronics" in *Quantum Effects in Small Disordered Systems*, ed. by B. L. Al'tshuler, P. A. Lee, and R. A. Webb (Elsevier, Amsterdam, 1990).

G. Schön and A. D. Zaikin, Phys. Rep. **198**, 237 (1990).

[2] K. K. Likharev, IEEE Trans. Mag. MAG-23, 1142 (1987); Sov. Microelectron. **16**, 195 (1987).

[3] Yu. V. Nazarov, Sov. Phys. JETP **68**, 561 (1989); JETP Lett. **49**, 126 (1989).

[4] M. H. Devoret, D. Esteve, H. Grabert, G.-L. Ingold, H. Pothier, and C. Urbina, Phys. Rev. Lett. **64**, 1824 (1990).

[5] S. M. Girvin, L. I. Glazman, M. Jonson, D. R. Penn, and M. D. Stiles, Phys. Rev. Lett. **64**, 3183 (1990).

[6] G. Schön, LT-19 Satellite Workshop on Macroscopic Quantum Phenomena, ed. by T. D. Clark (World Scientific, Singapore, 1990).

[7] For reviews, see

M. Büttiker and R. Landauer, IBM J. Res. Dev. **30**, 451 (1986).

E. H. Hauge and J. A. Støvneng, Rev. Mod. Phys. **61**, 917 (1989).

[8] C. A. Neugebauer and M. B. Webb, J. Appl. Phys. **33**, 74 (1962).

[9] I. Giaever and H. R. Zeller, Phys. Rev. Lett. **20**, 1504 (1968); Phys. Rev. **181**, 789 (1969).

[10] J. Lambe and R. C. Jaklevic, Phys. Rev. Lett. **22**, 1371 (1969).

[11] R. E. Cavicchi and R. H. Silsbee, Phys. Rev. Lett. **52**, 1453 (1984).

[12] D. V. Averin and K. K. Likharev, J. Low Temp. Phys. **62**, 345 (1986).

[13] L. S. Kuzmin and K. K. Likharev, JETP Lett. **45**, 389 (1987).

[14] T. A. Fulton and G. J. Dolan, Phys. Rev. Lett. **59**, 109 (1987).

[15] J. B. Barner and S. T. Ruggiero, Phys. Rev. Lett. **59**, 807(1987).

[16] L. S. Kuzmin, P. Delsing, T. Claeson, and K. K. Likharev, Phys. Rev. Lett. **62**, 2539 (1989).

[17] P. J. M. van Bentum, H. van Kempen, L. E. C. van de Leemput, and P. A. A. Teunissen, Phys. Rev. Lett. **60**, 369 (1988).

[18] R. Wilkins, E. Ben-Jocob, and R. C. Jaklevic, Phys. Rev. Lett. **63**, 801 (1989).

[19] D. V. Averin, Sov. J. Low. Temp. Phys. **13**, 208 (1987).

[20] E. Ben-Jacob. Y. Gefen, K. Mullen and Z. Schuss, Phys. Rev. B, **37**, 7400 (1988).

[21] K. Mullen, Y. Gefen, and E. Ben-Jacob, Physica B+C **152B**, 172 (1988).

[22] U. Gegenmüller and G. Schön, Physica B+C **152B**, 186 (1988).

[23] M. Ueda and Y. Yamamoto, Phys. Rev. B **41**, 3082 (1990).

[24] M. Ueda, Phys. Rev. B **42**, 3087 (1990).

[25] M. Ueda, Physica B **165** & **166**, 981 (1990).

[26] M. Ueda and N. Hatakenaka, Phys. Rev. B **43**, (1991).

[27] P. Delsing, K. K. Likharev, L. S. Kuzmin, and T. Claeson, Phys. Rev. Lett. **63**, 1180 (1989).

[28] P. Delsing, K. K. Likharev, L. S. Kuzmin, and T. Claeson, Phys. Rev. Lett. **63**, 1861 (1989).

[29] A. N. Cleland, J. M. Schmidt, and J. Clarke, Phys. Rev. Lett. **64**, 1565 (1990).

[30] M. Ueda and S. Kurihara, Proc. LT-19 Satellite Workshop on Macroscopic Quantum Phenomena, ed. by T. D. Clark (World Scientific, Singapore, 1990).

[31] M. Ueda and S. Kurihara, Phys. Rev. Lett. (submitted).

[32] The only remnant of the discreteness of tunneling events is seen in the Schottky formula, where the tunneling-current spectrum $S_I(\omega) = \frac{1}{2\pi} eI$ is proportional to the quantized unit of electricity e.

[33] C. B. Duke, *Tunneling in Solids*, edited by E. Burnstein and S. Lundqvist (Plenum, New York, 1968).

[34] T. Claeson, P. Delsing, L. S. Kuzmin and K. K. Likharev, Proc. 3rd Int. Symp. Foundation of Quantum Mechanics (Tokyo, 1989), p.255.

[35] W. Heisenberg, *Physical Principles of the Quantum Theory* (Dover, 1930).

[36] Y. Srivastava and A. Widom, Phys. Rep. **148**, 1 (1987).

[37] E. Arthurs and J. L. Kelly, Jr., Bell Syst. Tech. J. **44**, 725 (1965).

[38] A. J. Leggett, Phys. Rev. **B30**, 1208 (1984).

[39] C. Kittel, *Quantum theory of solids* (Wiley, New York, 1963), Chap. 20.

[40] Y. Aharonov and D. Bohm, Phys. Rev. **122**, 1649 (1961).

[41] M. Ueda, Phys. Rev. A **38**, 2937 (1988); ibid. **40**, 1096 (1989).

[42] P. Nozières and C. T. De Dominicis, Phys. Rev. **178**, 1097 (1969).

[43] G. Yuval and P. W. Anderson, Phys. Rev. B **1**, 1522 (1970).

[44] The physical reason for this is that two types of singular bubbles appear simultaneously in *irreducible* graphs when we expand the response function of the tunneling Hamiltonian by an ordinary perturbation technique. In such cases we must sum, even in the lowest order, the "parquet" graphs instead of the ladder graphs. See A. A. Abrikosov, Physics **2**, 5 (1965).

[45] R. Kubo, J. Phys. Soc. Jpn. **12**, 570 (1957).

[46] T. -L. Ho, Phys. Rev. Lett. **51**, 2060 (1983).

[47] E. Ben-Jacob, E. Mottola, and G. Schön, Phys. Rev. Lett. **51**, 2064 (1983).

[48] E. Müller-Hartmann, T. V. Ramakrishnan, and G. Toulouse, Phys. Rev. **B3**, 1102 (1971).

[49] M. Abramowitz and I. A. Stegun (eds.), *Handbook of Mathematical Functions with Formulas, Graphs, and Mathematical Tables* (National Bureau of Standards, Applied Mathematics Series 55, 1972).

Figure captions

Fig. 1 Principle of Coulomb blockade: (a) An electron can pass through the energy barrier owing to the wave nature of an electron, (b) but each tunneling event is accompanied by an energy cost of $\frac{e}{c}\left(\frac{e}{2}-Q\right)$ due to the particle nature (quantization of charge) of an electron.

Fig. 2 Principle of single-electron-tunneling oscillations: (a) A current-driven small tunnel junction; (b) inhibition of tunneling due to Coulomb blockade (c) charge (voltage) oscillations (solid line) and associated quantization of tunneling current (shaded pulses).

Fig. 3 Physical meaning of the fractional charge Q: it is proportional to the relative displacement between the center of mass of the whole conduction electrons and that of the whole positive ions.

Fig. 4 Schematic illustrations of (a) a current-biased tunnel junction with stray capacitance C_S and inductance L, and (b) a voltage-biased tunnel junction.

Fig. 5 (a) Voltage-biased tunnel junction with a source resistance connected in series in it. (b) Current-biased tunnel junction with a shunt resistance connected in parallel to it.

Fig. 6 (a) Time intervals between consecutive tunneling events. (b) Definition of time-interval distribution. (c) Time-interval distribution for regular and random tunneling events.

Fig. 7 Time development of the accumulated charge on the junction, where Q_i and Q_f denote the initial charge and final charge.

Fig. 8 Initial-charge distributions (a)-(d) and final-charge distributions (e)-(h) for (a),(e) $\frac{R_S}{R_T}=300$, (b),(f) $\frac{R_S}{R_T}=100$, (c),(g) $\frac{R_S}{R_T}=10$, and (d),(h) $\frac{R_S}{R_T}=1$ with $CV=e$.

Fig. 9 Time-interval distributions for (a) $\frac{R_S}{R_T}=300$, (b) $\frac{R_S}{R_T}=100$, (c) $\frac{R_S}{R_T}=10$, and (d) $\frac{R_S}{R_T}=1$ with $CV=e$, where the time axis is normalized by CR_S.

Fig. 10 Charge distribution for (a) $\frac{R_S}{R_T}=300$, (b) $\frac{R_S}{R_T}=100$, (c) $\frac{R_S}{R_T}=10$, and (d) $\frac{R_S}{R_T}=1$ with $CV=e$.

Fig. 11 Normalized degree of randomness as a function of the ratio $\frac{R_S}{R_T}$ for several values of the product CV. The ordinate is normalized by the standard quantum limit, where the constant current I_{dc} needed to calculate the standard quantum limit is set equal to the average current which is actually obtained by computer simulation for the corresponding value of the ratio $\frac{R_S}{R_T}$.

Fig. 12 Schematic of a normal tunnel junction. A tunneling event produces a sudden change in the localized Coulomb potential on either side of the barrier.

Fig. 13 Disentanglement of many-body time-independent graphs to one-body time-dependent graphs. (a) A typical many-body graph represented by the Hamiltonian (6.1)-(6.5). (b) Reduced one-body graph, where time-dependence appears only as a boundary condition.

Fig. 14 Schematic illustration describing the effect of the Fermi-surface environment on tunneling.

Fig. 15 Contour for integral (D.3)

Fig. 16 Contour for integral (D.8)

Fig. 1

(a)

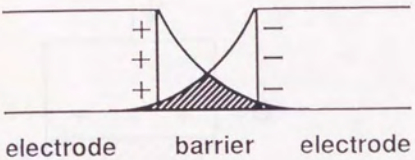

(b)

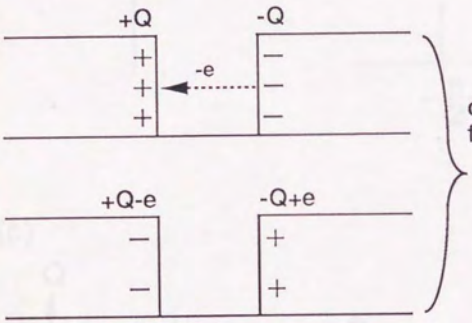

change in the Coulomb energy for a single-electron tunneling

$$\Delta E = \frac{e}{C}\left(\frac{e}{2} - Q\right)$$

Fig. 2

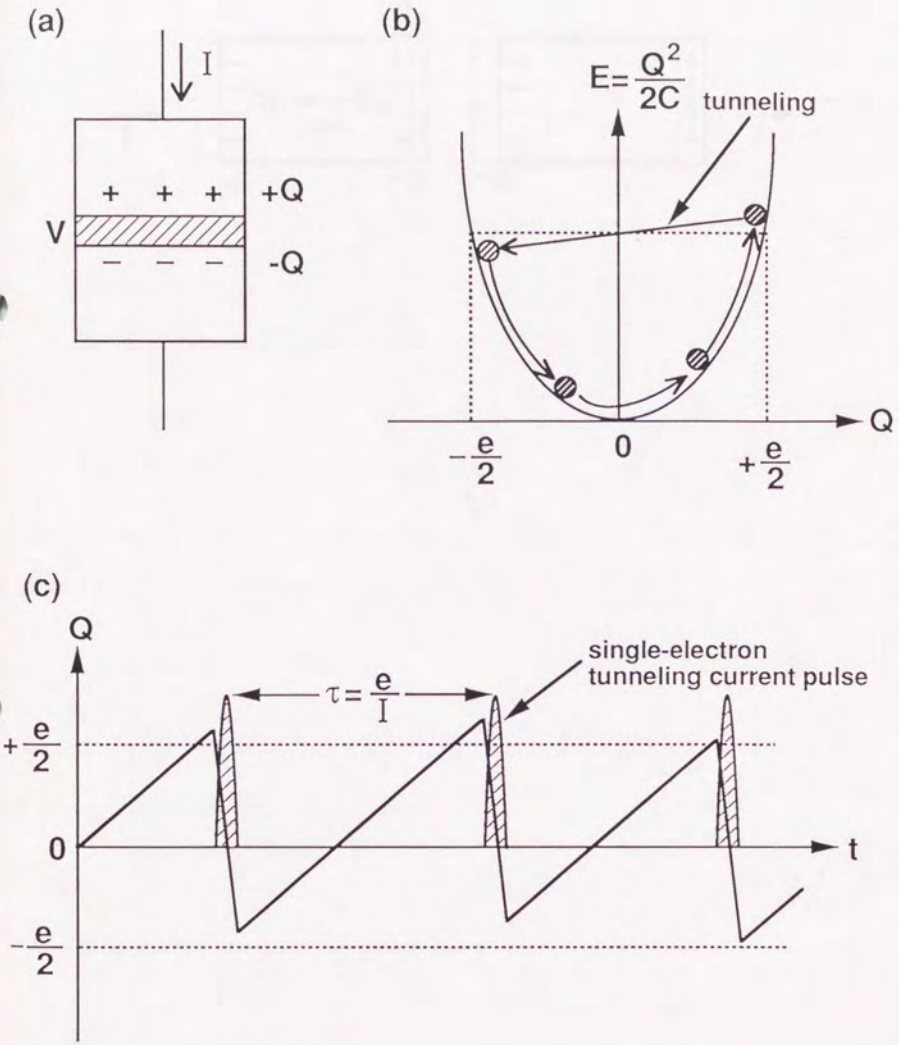
(a)
I
+ + +
+Q
V
− − −
-Q
(b)
E= Q²/2C
tunneling
Q
−e/2
0
+e/2
(c)
Q
single-electron
tunneling current pulse
τ= e/I
+e/2
0
−e/2
t

Fig. 3

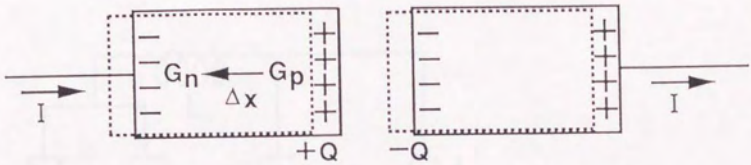

Fig. 4

(a)

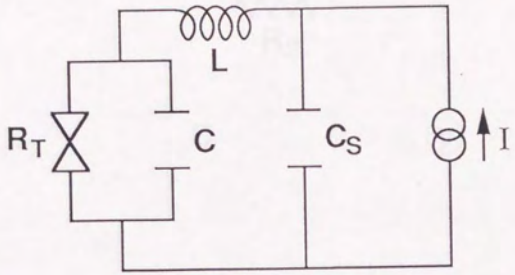

(b)

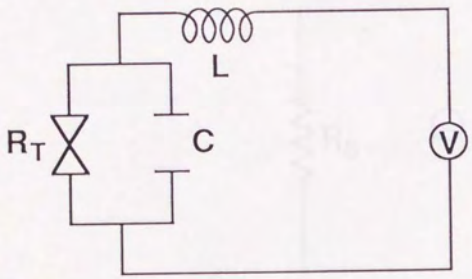

Fig. 5

(a)

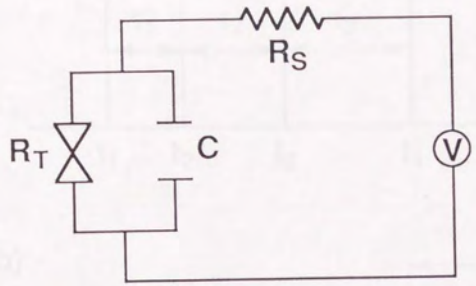

(b)

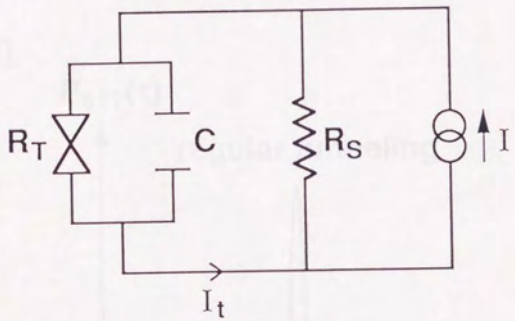

Fig. 6

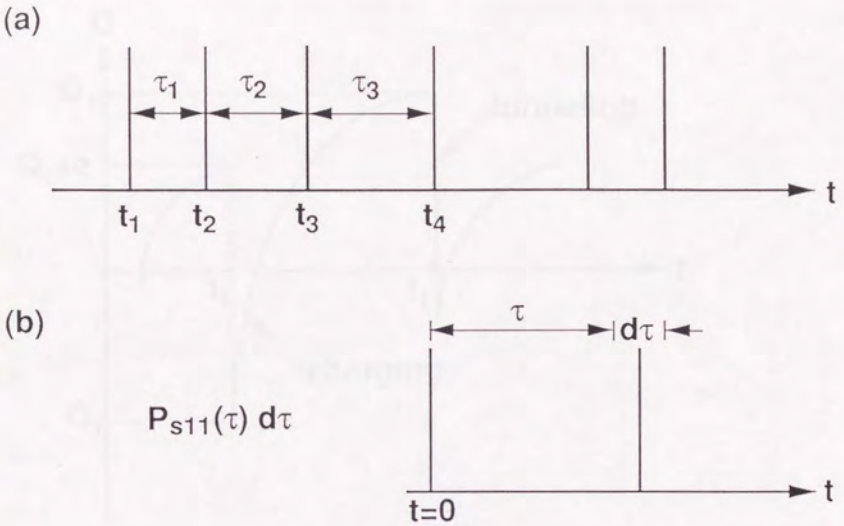
(a)
τ_1
τ_2
τ_3
t
t_1
t_2
t_3
t_4
(b)
τ
$d\tau$
$P_{s11}(\tau)\, d\tau$
t
t=0
(c)
$P_{s11}(\tau)$
regular tunneling
random tunneling
τ

Fig. 7

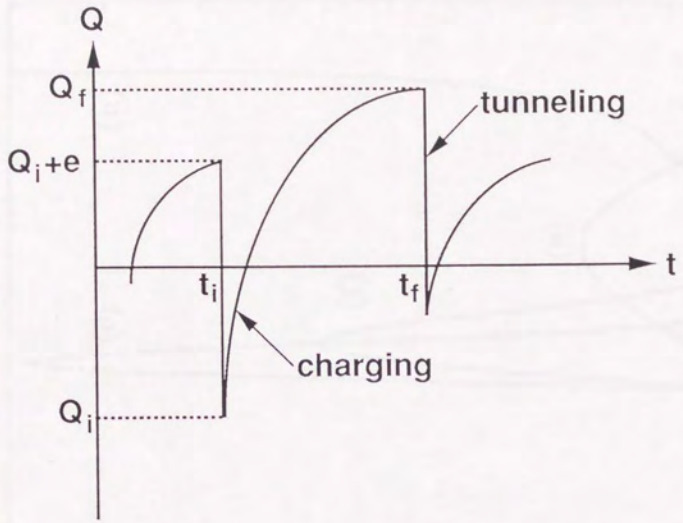

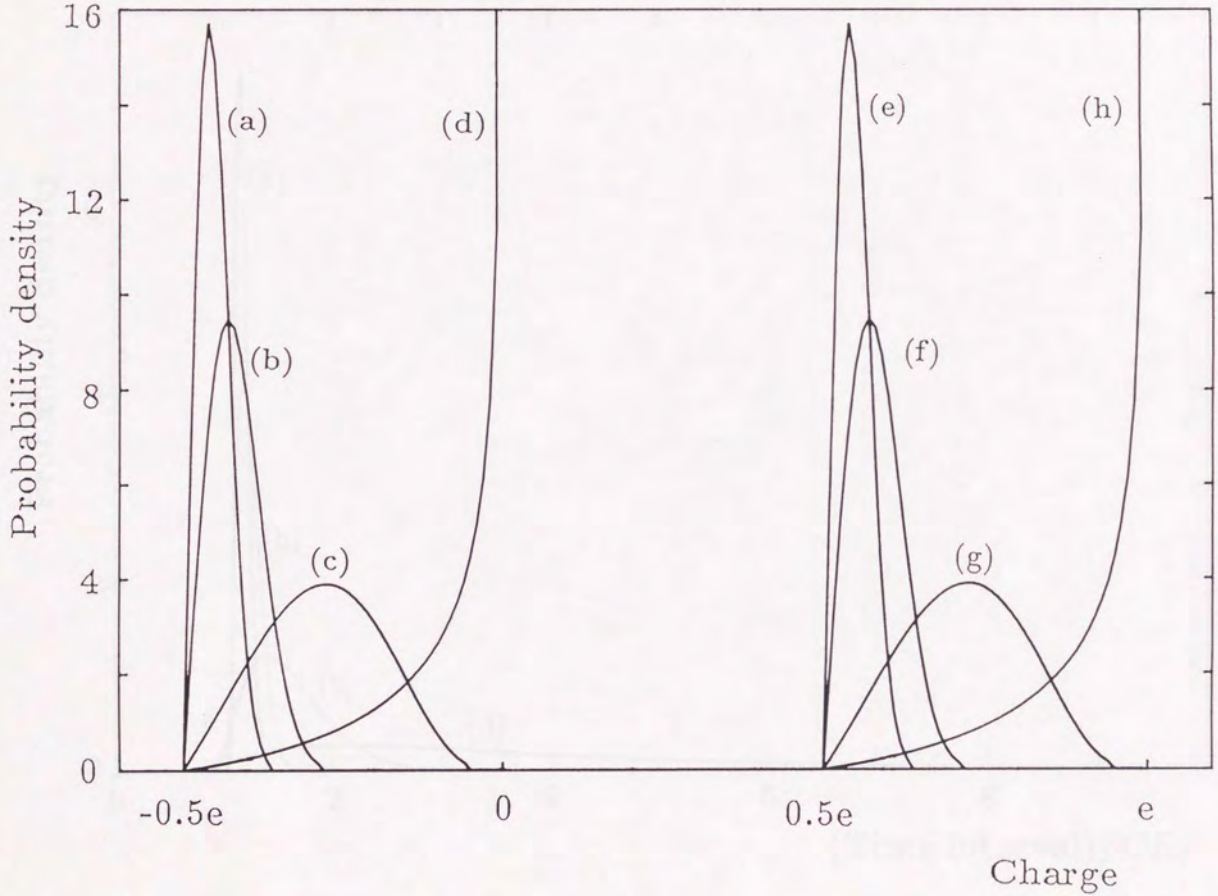

Fig. 8

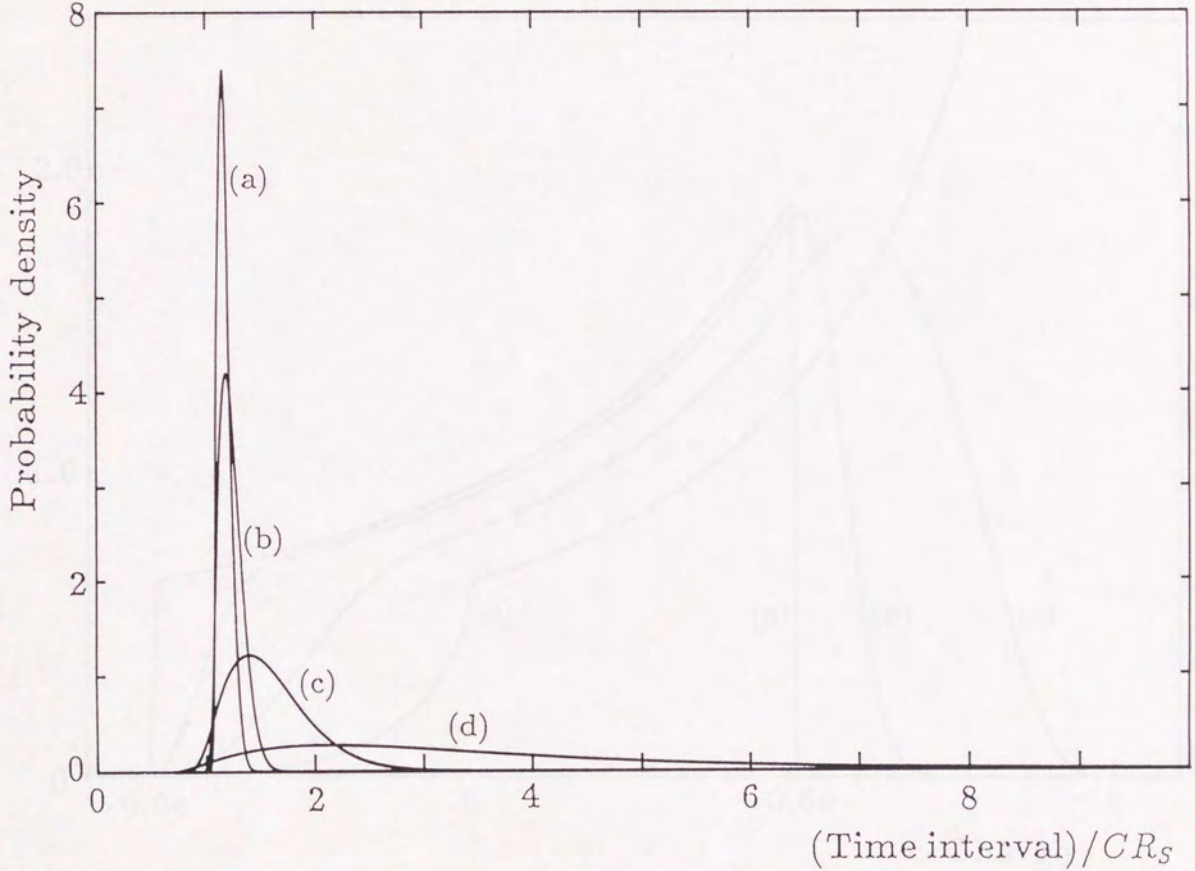

Fig. 9

Fig. 10

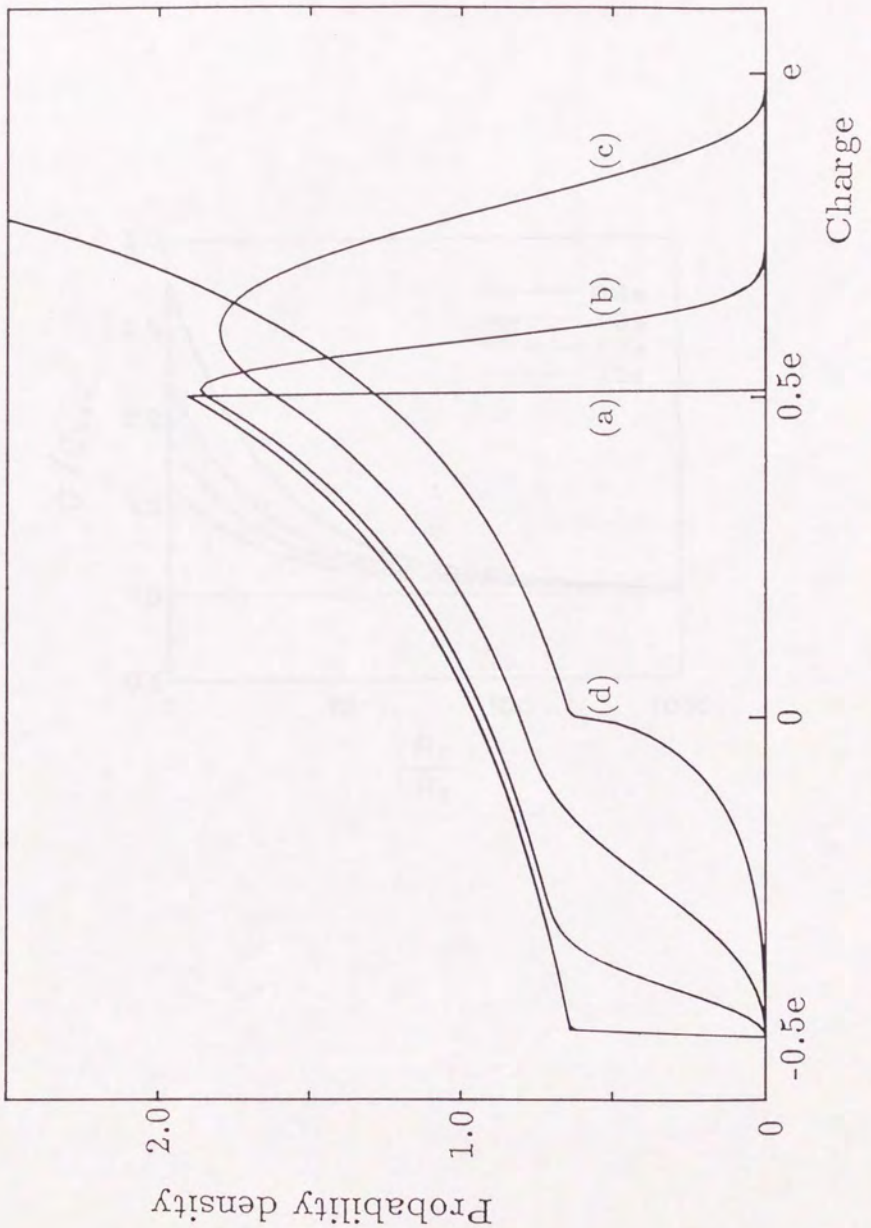

Fig. 11

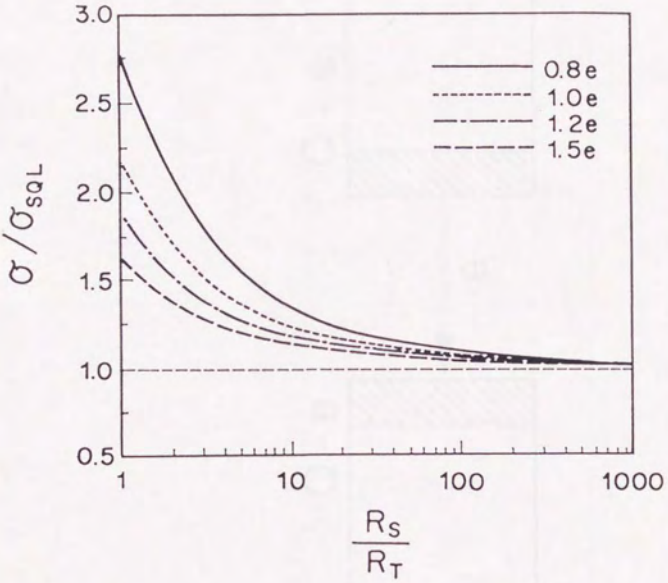

Fig. 12

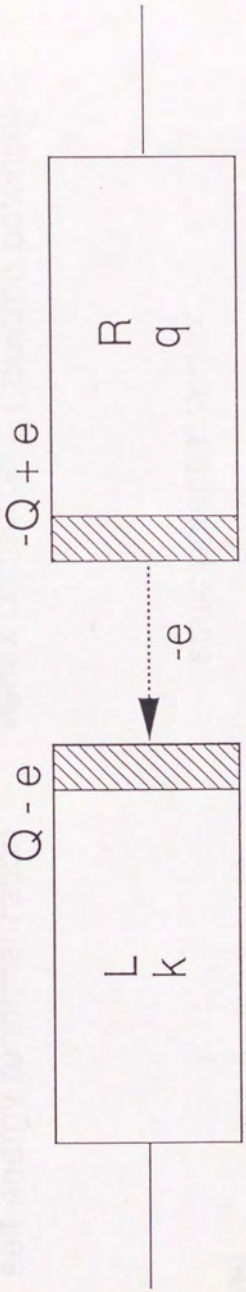

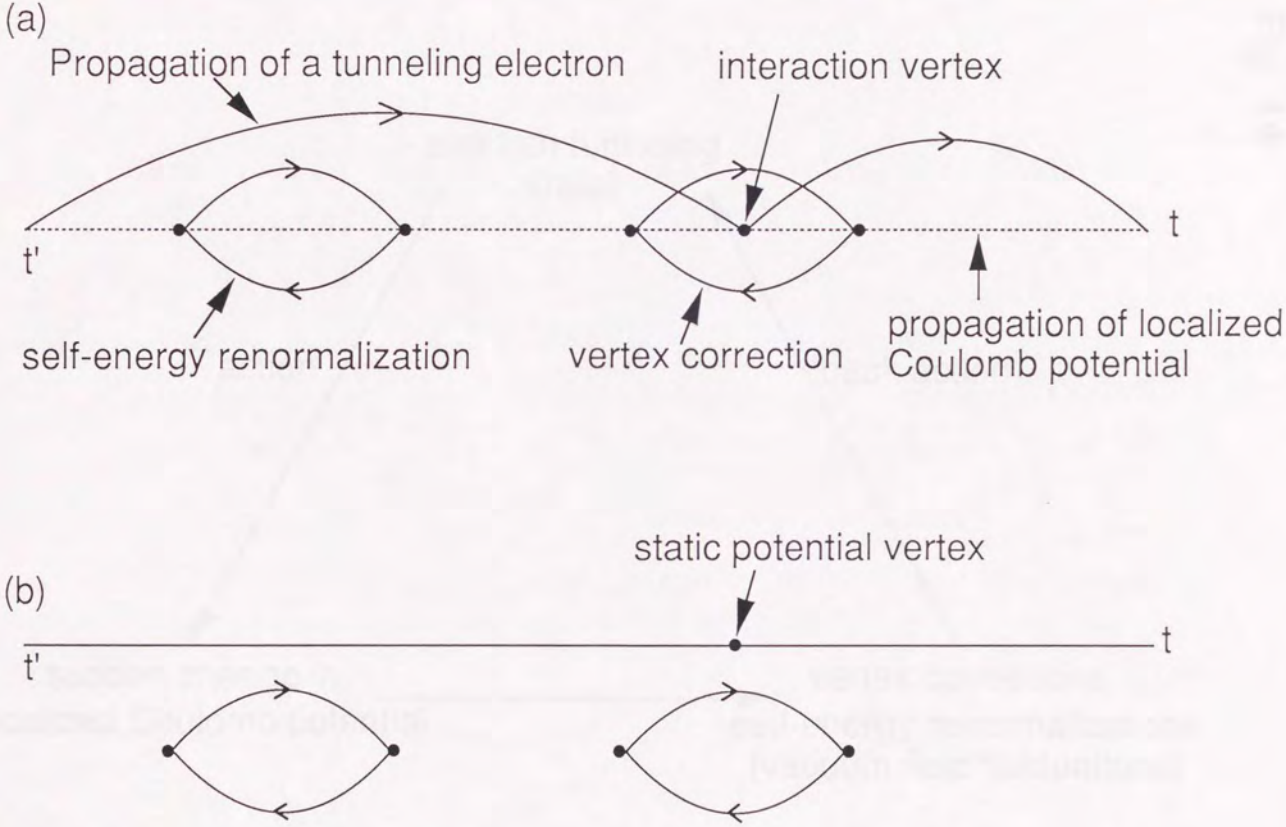
(a)
Propagation of a tunneling electron
interaction vertex
t
t'
self-energy renormalization
vertex correction
propagation of localized
Coulomb potential
(b)
static potential vertex
t
t'

Fig. 13

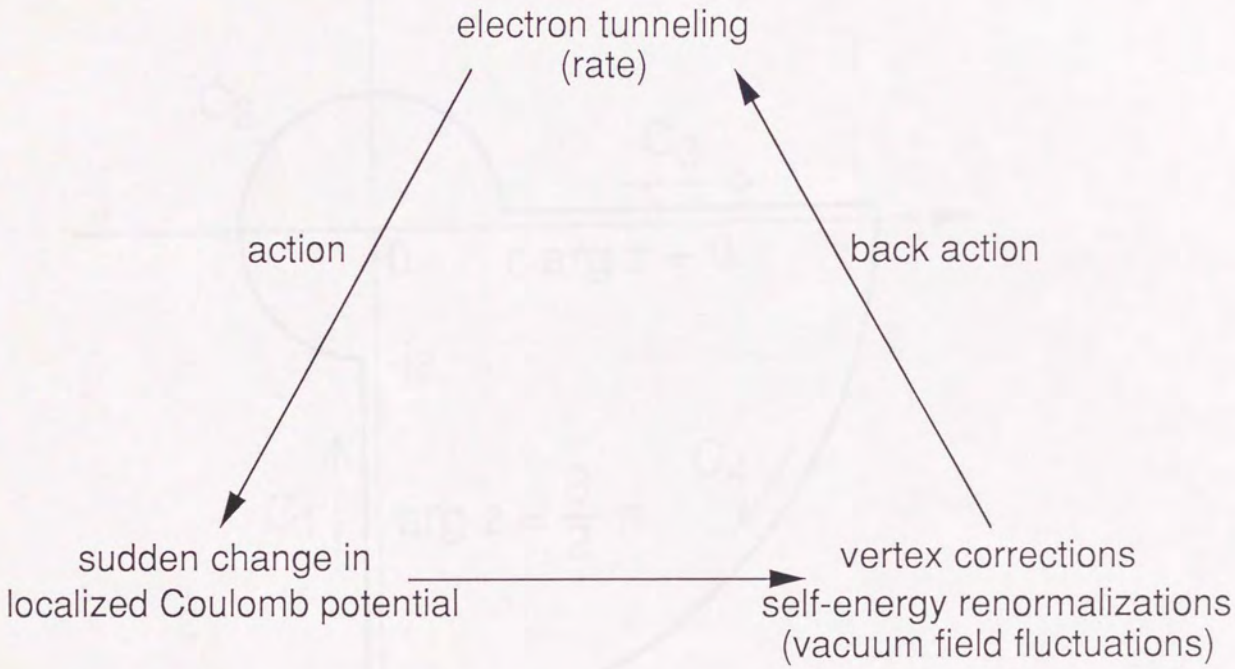
electron tunneling
(rate)
action
back action
sudden change in
localized Coulomb potential
vertex corrections
self-energy renormalizations
(vacuum field fluctuations)

Fig. 14

Fig. 15

complex z plane
C_3
ε arg z = 0
C_4
$\arg z = \frac{3}{2}\pi$
0
-iε
C_2
C_1

Fig. 16

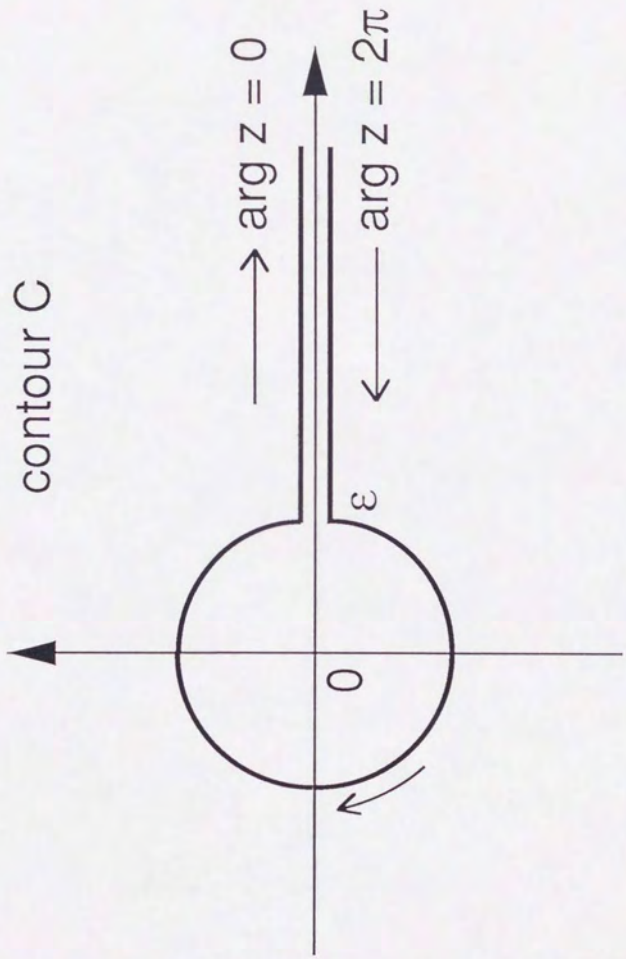

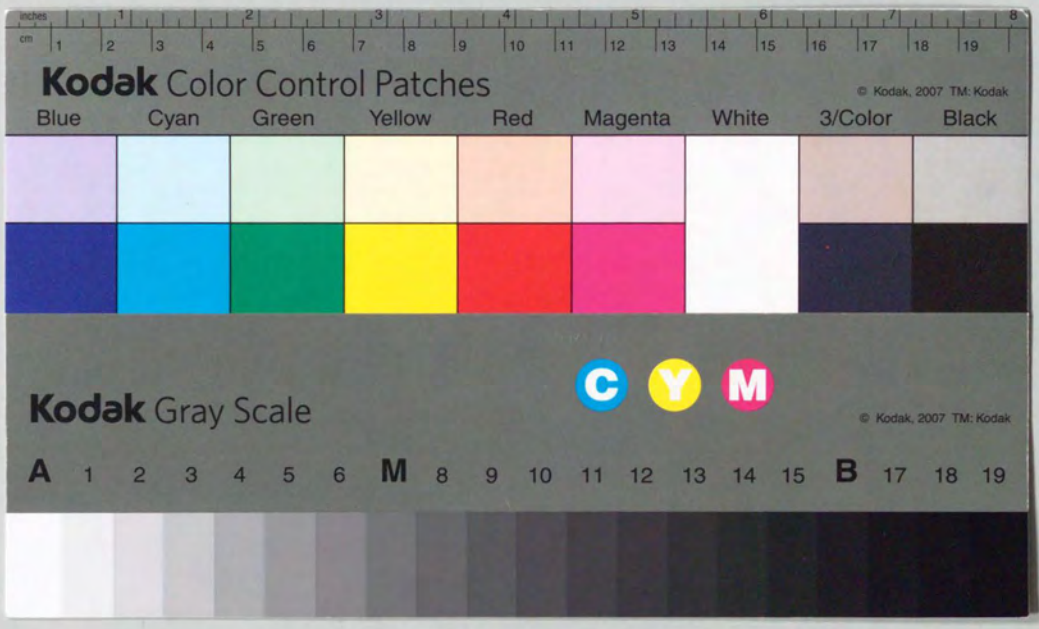
inches
cm
Kodak Color Control Patches
© Kodak, 2007 TM: Kodak
Blue
Cyan
Green
Yellow
Red
Magenta
White
3/Color
Black
Kodak Gray Scale
C
Y
M
© Kodak, 2007 TM: Kodak
A 1 2 3 4 5 6 M 8 9 10 11 12 13 14 15 B 17 18 19